

1 **Trait components of whole plant water use efficiency are defined by unique,**
2 **environmentally responsive genetic signatures in the model C₄ grass *Setaria***

3

4 Max J. Feldman¹, Patrick Z. Ellsworth², Noah Fahlgren¹, Malia A. Gehan¹, Asaph B.
5 Cousins² and Ivan Baxter^{1,3,*}

6

7 *Corresponding author

8 E-mail: ivan.baxter@ars.usda.gov (IB)

9

10 ¹Donald Danforth Plant Science Center, St. Louis, Missouri, USA

11 ²School of Biological Sciences, Washington State University, Pullman, Washington,
12 USA

13 ³USDA-ARS, Plant Genetics Research Unit, St. Louis, Missouri, USA

14

15 **ABSTRACT**

16 Plant growth and water use are interrelated processes influenced by the
17 genetic control of both plant morphological and biochemical characteristics.
18 Improving plant water use efficiency (WUE) to sustain growth in different
19 environments is an important breeding objective that can improve crop yields and
20 enhance agricultural sustainability. However, genetic improvements of WUE using
21 traditional methods have proven difficult due to low throughput and environmental
22 heterogeneity encountered in field settings. To overcome these limitations the study
23 presented here utilizes a high-throughput phenotyping platform to quantify plant
24 size and water use of an interspecific *Setaria italica* x *Setaria viridis* recombinant
25 inbred line population at daily intervals in both well-watered and water-limited
26 conditions. Our findings indicate that measurements of plant size and water use in
27 this system are strongly correlated; therefore, a linear modeling approach was used
28 to partition this relationship into predicted values of plant size given water use and
29 deviations from this relationship at the genotype level. The resulting traits
30 describing plant size, water use and WUE were all heritable and responsive to soil
31 water availability, allowing for a genetic dissection of the components of plant WUE

32 under different watering treatments. Linkage mapping identified major loci
33 underlying two different pleiotropic components of WUE. This study indicates that
34 alleles controlling WUE derived from both wild and domesticated accessions of the
35 model C₄ species *Setaria* can be utilized to predictably modulate trait values given a
36 specified precipitation regime.

37

38 **INTRODUCTION**

39 Improving crop productivity while simultaneously reducing agricultural
40 water input is essential to ensure the security of our global food supply and protect
41 our diminishing fresh water resources. Agriculture is by far the greatest industrial
42 consumer of fresh water, largely because productivity losses related to drought
43 stress can decrease crop yields by greater than 50% (Boyer, 1982; Hamdy et al.,
44 2003). Addressing these challenges will require an integrated approach that
45 combines irrigation practices that minimize water loss and deployment of crop
46 plants with superior water use efficiency (Boutraa, 2010; Davies and Bennett, 2015;
47 Evans and Sadler, 2008; Gregory and George, 2011; Morison et al., 2008; Stanhill,
48 1986).

49 Plant water use efficiency (WUE) can be broadly defined as the ratio of
50 biomass produced to total water lost by the plant (Bacon, 2009; Blum, 2009;
51 Condon, 2004; Evans and Sadler, 2008; Monteith, 1993; Morison et al., 2008;
52 Tardieu, 2013). This complex trait is determined by many factors including
53 photosynthetic carbon assimilated per unit of water transpired (Condon et al., 2002;
54 Farquhar et al., 1989; Morison et al., 2008; Penman and Schofield, 1951; Seibt et al.,
55 2008), leaf architecture (Brodribb et al., 2007; Sack and Holbrook, 2006), stomata
56 characteristics (Franks and Farquhar, 2006; Lawson and Blatt, 2014), epidermal
57 wax content (Premachandra et al., 1994), canopy and root architecture (White and
58 Snow, 2012; Martre et al., 2001), stomatal dynamics (Blatt, 2000; Hetherington and
59 Woodward, 2003; Lawson et al., 2010; Flood et al., 2011; Lawson et al., 2012) ,
60 hydraulic transport (Edwards et al., 2012; Holloway-Phillips and Brodribb, 2011),
61 portion of carbon lost from respiration (Escalona et al., 2012; Tomás et al., 2014)

62 and partitioning of photo-assimilate (Carmo-Silva et al., 2009; Chaves, 1991). Given
63 that plant species (Stewart et al., 1995; Winter et al., 2005; Zegada-Lizarazu and
64 Iijima, 2005; Zhou et al., 2012) and ecotypes within species (Kenney et al., 2014;
65 Lopez et al., 2015; Nakhforoosh et al., 2016; Pater et al., 2017; Ryan et al., 2016; Xu
66 et al., 2009) exhibit variation in WUE it is likely that the characteristics which
67 determine this trait are under genetic control and have evolved in response to
68 different environmental conditions such as water availability (Assouline and Or,
69 2013; Brodribb et al., 2009; Huxman et al., 2004). Therefore, WUE is likely
70 influenced by both genetically encoded developmental programs and changes in
71 growth environments throughout the plant lifecycle (Fleury et al., 2010).

72 The technical challenges associated with measuring plant size and
73 transpiration in large structured genetic populations has historically limited
74 experimental efforts aimed at identifying the genetic components associated with
75 WUE. This is particularly difficult in field settings due to year-to-year climate
76 fluctuation and micro-environmental variation observed within agricultural fields.
77 The advent of controlled environment, high-throughput phenotyping instruments
78 (Chen et al., 2014; Fahlgren et al., 2015; Granier et al., 2006; Pereyra-Irujo et al.,
79 2012; Reuzeau et al., 2006; Sadok et al., 2007; Tisné et al., 2013; Walter et al., 2007)
80 alleviates many of these challenges through stringent control of climatic variables
81 and automated, high-resolution measurement of plant size and evapotranspiration
82 across large breeding populations.

83 Evidence from studies conducted on both crop and model plants indicate that
84 the traits associated with WUE are heritable and largely polygenic, although
85 identifying the causal locus associated with differential performance has proven
86 difficult in crop plants due to plant size and genome complexity (Adiredjo et al.,
87 2014; Aparna et al., 2015; Chen et al., 2012; Coupel-Ledru et al., 2016; Honsdorf et
88 al., 2014; Parent et al., 2015; Schoppach et al., 2016; Xu et al., 2009). Utilization of
89 model plants (C_3 annuals *Arabidopsis thaliana* and *Brachypodium distachyon*) that
90 possess tractable genetic and experimental properties has enabled scientists to
91 identify QTL that contribute to WUE (Des Marais et al., 2016; Easlon et al., 2014;
92 Lowry et al., 2013; Mojica et al., 2016; Vasseur et al., 2014), a few of which have

93 been mapped to causal genes (Ruggiero et al., 2017). Species in the genus *Setaria*
94 also possess many of these desirable qualities and can be used as experimental
95 models to identify genetic components associated with WUE in a C₄ plant that is
96 closely related evolutionarily to C₄ crops like maize, sorghum and bioenergy grasses
97 (Bennetzen et al., 2012; Brutnell et al., 2010; Huang et al., 2016; Li and Brutnell,
98 2011; Zhu et al., 2017). However, in order to study the diversity of resource
99 utilization tactics present in natural and mapping populations of *Setaria* (Saha et al.,
100 2016) or other C₄ plant species, methods to quantify plant performance and WUE
101 in different environments must be developed.

102 The objectives of this study were to use a controlled environment high-
103 throughput phenotyping system to characterize the genetic architecture of plant
104 size, water use and WUE in an interspecific *Setaria* recombinant inbred population
105 (RIL) under two different watering regimes. Our findings indicate that plant size,
106 water use and WUE are polygenic traits which are influenced by both soil water
107 content and greater than 10 pleiotropic loci whose effect size changes differentially
108 throughout development. In addition, we identify and discuss several aspects of
109 experimental design that should be considered when performing high-throughput
110 phenomics experiments to study plant WUE.

111

112 **MATERIALS AND METHODS**

113 *Plant material and growth conditions*

114 The experiment here was first described in (Feldman et al., 2017), which
115 focused on plant height, and the details are repeated here in quotes for clarity. “An
116 interspecific *Setaria* F7 RIL population comprised of 189 genotypes (1138
117 individuals) was used for genetic mapping. The RIL population was generated
118 through a cross between the wild-type green foxtail *S. viridis* accession, A10, and the
119 domesticated *S. italica* foxtail millet accession, B100 (Bennetzen et al., 2012; Devos
120 et al., 1998; Wang et al., 1998). After a six-week stratification in moist long fiber
121 sphagnum moss (Luster Leaf Products Inc., USA) at 4°C, *Setaria* seeds were planted
122 in 10 cm diameter white pots pre-filled with ~470 cm³ of Metro-Mix 360 soil
123 (Hummert, USA) and 0.5 g of Osmocote Classic 14-14-14 fertilizer (Everris, USA).

124 After planting, seeds were given seven days to germinate in a Conviron growth
125 chamber with long day photoperiod (16 h day/8 h night; light intensity
126 $230 \mu\text{mol}/\text{m}^2/\text{s}$) at 31°C day/ 21°C night before being loaded onto the Bellwether
127 Phenotyping System using a random block design. Plants were grown on the system
128 for 25 days under long day photoperiod (16 h day/8 h night; light intensity 500
129 $\mu\text{mol}/\text{m}^2/\text{s}$) with the same temperature regime used during germination. Relative
130 humidity was maintained between 40 – 80 %. Gravimetric estimation of pot weight
131 was performed 2-3 times per day and water was added to maintain soil volumetric
132 water content at either 33% full-capacity (FC) (water-limited) or 100% FC (well-
133 watered) as determined by (Fahlgren et al., 2015). Prescribed soil water content
134 across both treatment blocks was achieved by 15 days after planting (DAP).

135 The volume of water transpired by individual plants at each pot weighing
136 was calculated as the difference between the measured pot weight and the weight of
137 the pre-filled pot at pot capacity (100% FC) or the difference between current pot
138 weight and the previous weight measurement if no water was added. At the
139 conclusion of each weighing, if the pot weight was below the set point, water was
140 added to the pot to return soil water content back to its target weight. This strategy
141 effectively maintains soil moisture content at a consistent level within both
142 treatment blocks. To evenly establish seedlings before the water limitation
143 treatment began, equal volumes of water (100% FC) were added to all pots for two
144 days after transfer to the system. At 10 DAP, a dry down phase was initiated (no
145 watering) to establish the water-limited treatment block (40% FC) while continuing
146 to maintain a soil water content of 100% FC within the well-watered treatment
147 block.”

148

149 *Image acquisition and derived measurements*

150 RGB images of individual plants were acquired using a top-view and a side-
151 view cameras at four different angular rotations (0° , 90° , 180° , 270°) every other day
152 at the Bellwether Phenotyping Facility (Fahlgren et al., 2015). Optical zoom was
153 adjusted throughout the experiment to ensure accurate quantification of traits
154 throughout plant development. The unprocessed images and the details of the

155 configuration settings can be found at the following download site:
156 (https://plantcv.danforthcenter.org/pages/data-sets/setaria_height.html).
157 Plant objects were extracted from images and analyzed using custom PlantCV
158 Python scripts specific to each camera (side-view or top-view), zoom level, and lifter
159 height (https://github.com/maxjfeldman/Feldman_Elsworth_Setaria_WUE_2017).
160 Scaling factors relating pixel area and distance to ground truth measurements
161 calculated by (Fahlgren et al., 2015) were used to translate pixels to relative area
162 (pixels/cm²) and relative distance (pixels/cm).

163

164 *Biomass estimation*

165 At the conclusion of the experiment, 176 individual plants (91 plants from
166 the 100% FC and 85 from the 40% FC) were harvested to measure aboveground
167 biomass. Gravimetric measurement of fresh weight and saturated fresh weight were
168 taken directly upon tissue harvest after which plant tissue was placed into
169 polypropylene micro-perforated bags (PJP MarketPlace #361001), dried for three
170 days at 60 °C and subsequently weighed to determine dry weight biomass.
171 Multivariate linear regression was used to evaluate, select and calibrate a predictive
172 model for fresh and dry weight plant biomass.

173 Regressing plant fresh weight biomass as a function of side-view area,
174 perimeter length, height, object solidity and width indicated that each of these terms
175 is a significant predictor of fresh weight biomass after stepwise model selection
176 using Akaike's Information Criterion (AIC) (Bozdogan, 1987); multiple R² = 0.89).
177 Unlike fresh weight biomass, side-view area, width, and height were the only
178 significant terms used for prediction of dry weight biomass after using the AIC
179 stepwise model selection correction procedure (multiple R² = 0.76). Models
180 containing all significant terms and their interaction achieved a greater model fit,
181 but they introduced artifacts at earlier developmental time points due to model
182 over-fitting (Fig. S1). Generally, models constructed to estimate fresh weight
183 biomass in the well-watered treatment block exhibited greater explanatory power
184 than those constructed to predict dry weight biomass or those in water-limited
185 treatment blocks (Fig. 1).

186 A minimal model containing only the most significant term (side-view area)
187 in both fresh and dry weight models produced a goodness of fit similar to more
188 complex models (fresh weight $R^2 = 0.86$; dry weight $R^2 = 0.74$). To avoid
189 propagation of error, values that incorporated plant fresh weight biomass were
190 calculated based on adjusted side-view pixel area and translated to fresh weight
191 biomass after analysis. Cumulative biomass values calculated on a genotype within
192 treatment basis were interpolated using loess smoothing (Chambers and Hastie,
193 1992). Plant size accumulation on a per day basis was calculated as the difference
194 between the loess fit values on a given day and the estimates from the previous day.

195

196 *Water loss tabulation*

197 The LemnaTec instrument at the Bellwether Phenotyping Facility provided
198 measurements of water use based upon the gravimetric weight of each pot before
199 watering, the volume of water applied, and the resulting weight after watering. On
200 days when the volume of water added to a pot was greater than zero, the daily
201 volume of water added was the sum of water volume added over a single calendar
202 day. On days when water was not added (e.g. during the dry down period), the
203 water volume was calculated as the minimum gravimetric weight of the pot on the
204 day in question subtracted from the minimum weight value from the previous day.
205 The cumulative volume of water used on a specific day was the sum of all water
206 used prior to that day. By fifteen days after planting (DAP), the dry down phase for
207 the water-limited treatment block was complete and pots containing plants lost
208 substantially more water than their empty pot counterparts in the well-watered
209 treatment block (Fig. 1). This observation indicates pot water loss cannot be
210 considered a proximity measure of total plant transpiration before day 15 in this
211 experiment (Fig. 1). Examination of the ratio between fresh weight biomass
212 accumulated relative to the amount of water used and mathematical prediction of
213 the amount of water used per day over this period suggests that the amount of
214 water used between day 15 and 17 can be used as an approximation of cumulative
215 water transpired by the plant throughout this experiment up to this point (Fig. S2).
216 This data and the observation that at day 17 the plants are still relatively small (less

217 than 8% of their maximum size on average) support the rationale of starting the
218 analysis on this day (Fig. 1). Volumes of water use (daily and cumulative) on a
219 genotype within treatment basis were estimated using loess smoothing.

220

221 *Heritability and trait variance partitioning*

222 We used the same approach as in (Feldman et al., 2017) and the details are
223 repeated here in quotes for clarity. “During this experiment, phenotypic values for
224 plant area and were calculated every other day, so the number of replicates per
225 treatment to calculate broad sense heritability was limited. To alleviate this
226 technical shortcoming, trait values for each individual were interpolated across
227 missing days using loess smoothing.

228 Variance components corresponding to broad sense heritability and total
229 variance explained was estimated using a mixed linear model using the R package
230 lme4 (Bates et al., 2015). Broad sense heritability was calculated using two
231 methods. Within an individual experiment, broad sense heritability on a line-
232 estimate basis was calculated using the following formula:

233

234 Equation 1:

$$235 \quad H^2_{\text{experiment}} = \sigma^2_{\text{genotype}} / (\sigma^2_{\text{genotype}} + (\sigma^2_{\text{genotype} \times \text{treatment}} / n_{\text{treatment}}) + (\sigma^2_{\text{residual}} /$$
$$236 \quad \quad \quad n_{\text{replicates}}))$$

237

238 in which $n_{\text{treatment}}$ is the harmonic mean of the number of treatment blocks in which
239 each line was observed and $n_{\text{replicates}}$ is the harmonic mean of number of replicates of
240 each genotype in the experiment. Heritability within treatment blocks was
241 calculated by fitting a linear model with genotype as the only explanatory factor
242 within each treatment block.

243

244 Equation 2:

$$245 \quad H^2_{\text{treatment block}} = \sigma^2_{\text{genotype}} / \sigma^2_{\text{total variance}}$$

246

247 The proportion of variance attributed to genotype divided by total variance
248 within each treatment block is reported as broad sense heritability within treatment
249 (equation). Total variance explained was calculated by fitting a linear model
250 including factors, genotype, treatment, plot and genotype x treatment effects across
251 all phenotypic values in all treatments. The proportion of variance that is
252 incorporated into these factors divided by the total variance in the experiment is
253 reported as total variance explained for each factor.”

254

255 *QTL analysis*

256 We used the same approach as in (Feldman et al., 2017) and the details are
257 repeated here in quotes for clarity. “QTL mapping was performed at each time point
258 within treatment blocks and on the numerical difference, relative difference and
259 trait ratio calculated between treatment blocks using functions encoded within the
260 R/qtl and funqtl package (Broman et al., 2003; Kwak et al., 2016). The functions
261 were called by a set of custom Python and R scripts
262 (https://github.com/maxjfeldman/foxy_qtl_pipeline). Two complimentary analysis
263 methods were utilized. First, a single QTL model genome scan using Haley-Knott
264 regression was performed to identify QTL exhibiting LOD score peaks greater than a
265 permutation based significance threshold ($\alpha = 0.05$, $n = 1000$). Next, a stepwise
266 forward/backward selection procedure was used to identify an additive, multiple
267 QTL model based upon maximization of penalized LOD score. Both procedures were
268 performed at each time point, within treatment blocks and on the numerical
269 difference relative difference and trait ratio calculated between phenotypic values
270 measured in treatment blocks at each time point. QTL associated with difference or
271 ratio composite traits may identify loci associated with genotype by environment
272 interaction (Des Marais et al., 2013).

273 The function-valued approach described by (Kwak et al., 2016), was used to
274 identify QTL associated with the average (SLOD) and maximum (MLOD) score at
275 each locus throughout the experiment. Each genotypic mean trait within treatments
276 was estimated using a logistic function, and the QTL significance threshold was
277 determined based upon permutation-based likelihood of observing the empirical

278 SLOD or MLOD test statistic. Separate, independent linkage mapping analysis
279 performed at each time point identified a larger number of QTL locations relative to
280 similar function valued analysis based on the SLOD and MLOD statistics calculated
281 at each individual marker throughout the experimental time course.
282 After refinement of QTL position estimates, the significance of fit for the full multiple
283 QTL model was assessed using type III analysis of variance (ANOVA). The
284 contribution of individual loci was assessed using drop-one-term, type III ANOVA.
285 The absolute and relative allelic effect sizes were determined by comparing the fit of
286 the full model to a sub-model with one of the terms removed. All putative protein
287 coding genes (*Setaria viridis* genome version 1.1) found within a 1.5-logarithm of
288 the odds (LOD) confidence interval were reported for each QTL.”

289

290 **RESULTS**

291

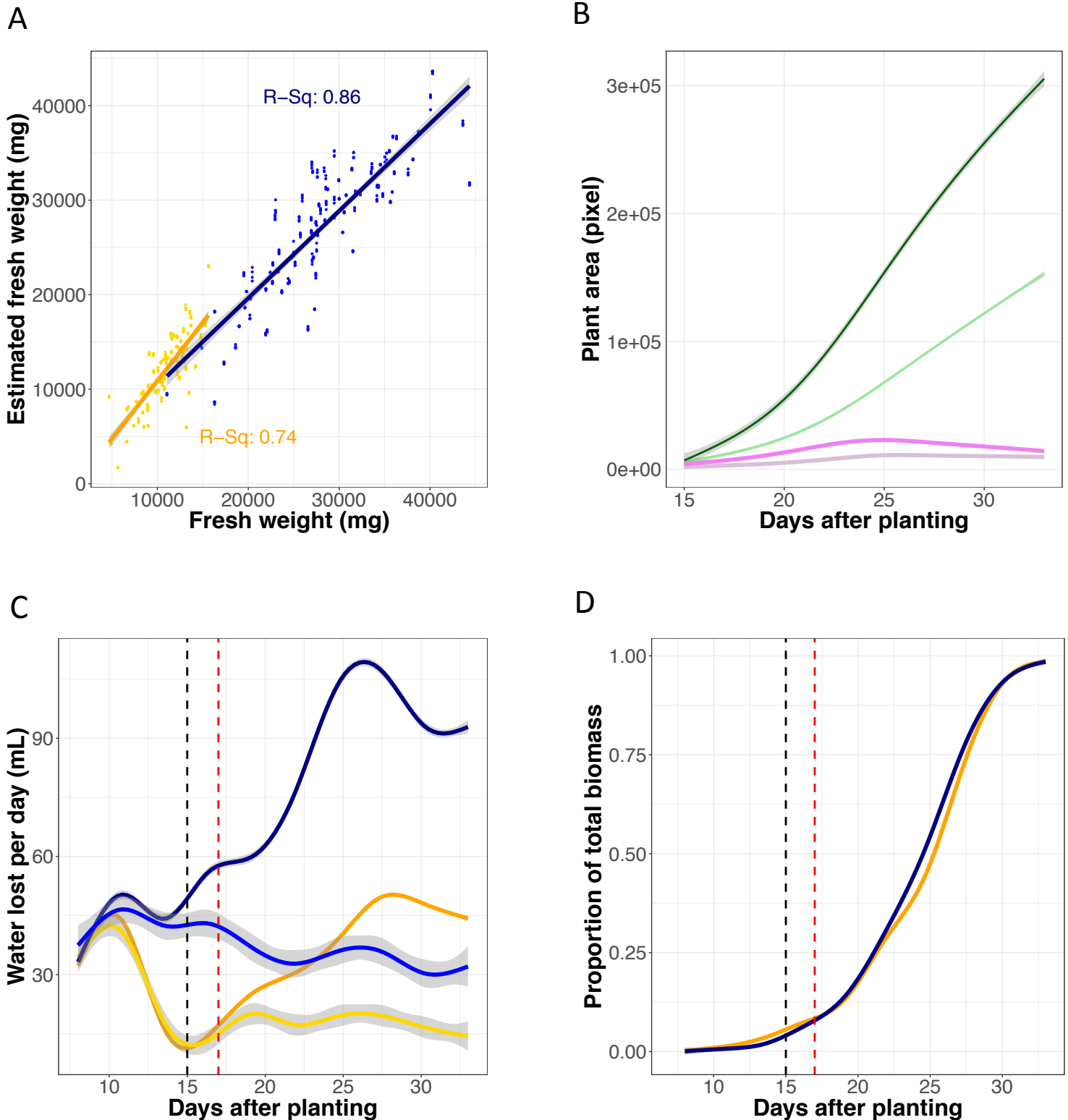
292 *Measuring plant size and water use throughout the plant lifecycle*

293 Recurrent measurement of plant size and water use was performed on
294 individuals of a *Setaria* recombinant inbred population (Devos et al., 1998; Devos et
295 al., 1998) grown at two soil water content levels at the Bellwether Phenotyping
296 Facility (Fahlgren et al., 2015). Images of each individual plant were captured every
297 other day from 7 to 33 days after sowing and plant objects were isolated and
298 quantified using PlantCV (Fahlgren et al., 2015; Feldman et al., 2017). Weight
299 estimates of fresh and dry-weight aboveground biomass were calculated using a
300 simple linear model featuring side-view area as the only predictor (Fig. 1, Fig. S3).

301 Daily plant water use was inferred through gravimetric measurement of pot
302 weight performed two to three times each day by the LemnaTec instrument. The
303 amount of water used by individual plants was calculated as the difference between
304 the measured weight of the pot and the weight of a pre-filled pot at a fixed point that
305 is proportional to its water holding capacity (100% FC) or the difference between
306 current weight and the previous weight measurement if no water was added. At the
307 conclusion of each weighing event, if pot weight was below the set point, water was
308 added to the pot to return it to the target weight value. This strategy effectively

Figure 1. Plant size and water use can be accurately inferred throughout a majority of the plant life cycle.

A) Significant correlations between plant fresh weight and pixel area were observed in both the well-watered and water-limited treatment blocks. B) Plants exhibited a sigmoidal growth curve, characterized by an average maximal rate of growth between 23–26 days after planting. Green lines reflect absolute average size, whereas purple lines report on growth rate. Dark and lighter shaded lines report the well-watered and water-limited treatment blocks respectively. C) Daily water loss can be accurately measured at 17 days after planting. Dark blue and orange lines correspond to average daily water lost from pots, whereas the lines with lighter shades of similar colors report the average water loss of empty pots. The dashed black line denotes the day at which dry down within the water-limited treatment block is complete whereas the dashed red line demarks when water use can be accurately measured. D) By 17 days after planting, plants have attained less than 8% of their total biomass.



309 maintains soil moisture potential at a consistent level within both treatment blocks.
310 To evenly establish seedlings before the water limitation treatment, equal volumes
311 of water (100% FC) were added to all pots for two days after transfer onto the
312 system. At 10 days after sowing, a dry down phase was initiated (no watering) to
313 establish uniformity within the water-limited treatment block (40% FC) while
314 continuing to maintain a soil water content of 100% FC within the well-watered
315 treatment block.

316 Examination of water loss from empty pots relative to those containing
317 plants suggested that early in the experiment a majority of water loss was
318 exclusively due to evaporation from the soil surface and did not informatively
319 report on plant transpiration (Fig. 1) (Ge et al., 2016). Beginning the analysis at day
320 17 enabled us to minimize the artifacts of evaporation that dominated early in the
321 experiment while still capturing growth attributes over a large proportion (~92%)
322 of the plant growth within the experiment (Fig. 1). Another potential confounding
323 issue was the use of a fixed set point for the pot weight, which neglected the
324 increasing weight of the plant when calculating the amount of water needed to
325 return the pot weight to the set point during watering jobs. This decreased the
326 volume of water present within each pot after watering by approximately 12.5%
327 (well-watered) and 17.5% (water-limited) on average by the end of the experiment
328 (Fig. S4).

329 Loess smoothing was used to interpolate the values of traits on a genotype
330 level within each treatment block across all experimental time points (Chambers
331 and Hastie, 1992). Rate statistics were calculated from these loess smoothed
332 estimates as the difference of the trait between days. Plots illustrating the mean and
333 variance of each trait can be observed in FIG. S5.

334

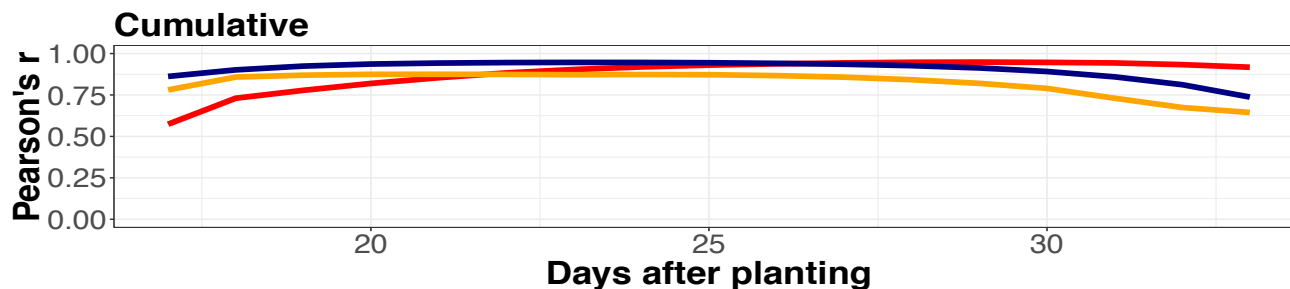
335 *Plant size and water use are correlated*

336 Over the course of this experiment cumulative plant size and water use were
337 highly correlated. Correlation was tightest between 21 and 27 DAP in the well-
338 watered treatment block (> 0.94) and quite strong between 20 and 27 DAP in the
339 water-limited treatment block (> 0.87, Fig. 2). In both treatment blocks, correlations

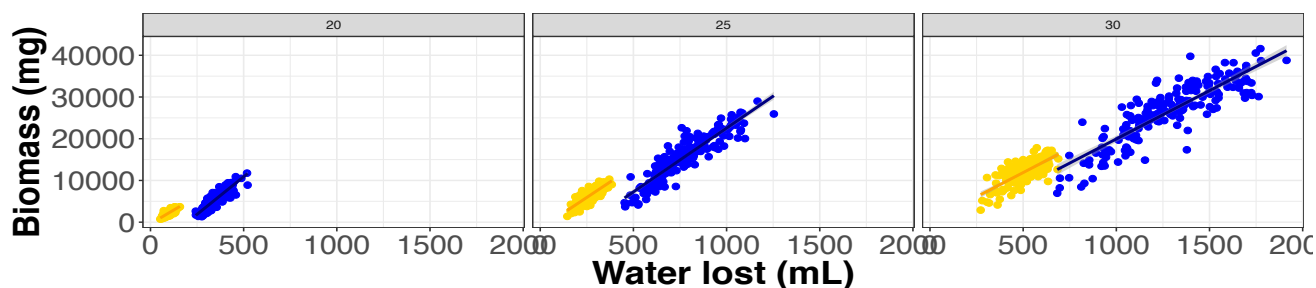
Figure 2. Plant size and water use are tightly correlated.

Pearson Correlation Coefficient both within (blue is well-watered, orange is water-limited) and between (red is across both) treatment blocks indicates strong correlation between these two characteristics, although the correlation between the rate of plant growth and daily water use decreases as plants approach maximum size. A) Correlation between cumulative plant size and water use. B) The relationship between plant size and water use at 20, 25 and 30 days after planting. C) Correlation between the rate of plant growth and daily water use. B) The relationship between plant growth rate and daily water use at 20, 25 and 30 days after planting.

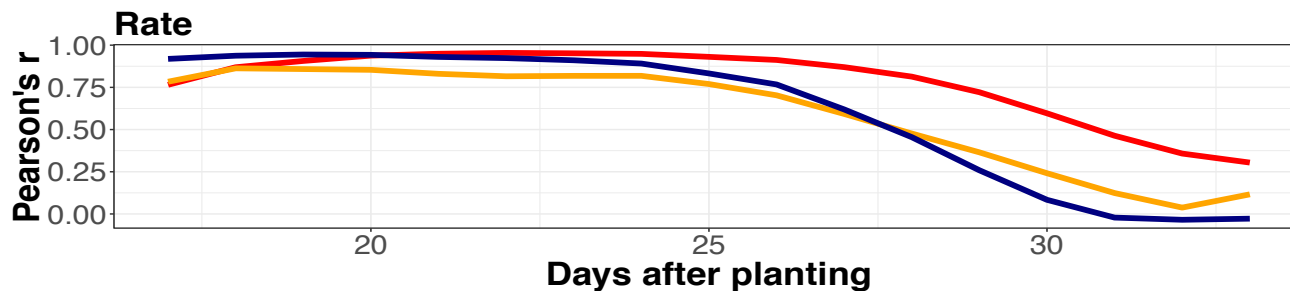
A



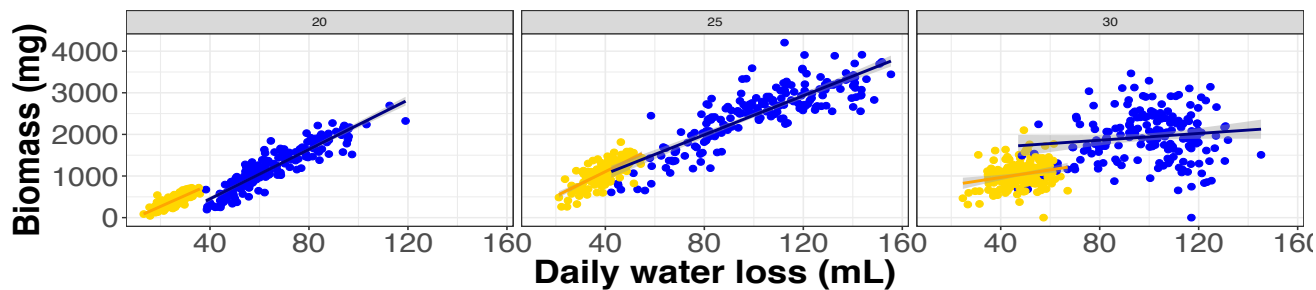
B



C



D



340 between these characters were weakest at the beginning and end of the experiment
341 but never dropped below 0.67. The correlation of the rate statistics associated with
342 these traits appeared qualitatively different. Correlation between plant growth rate
343 and the rate of water use was initially strong (> 0.79) but rapidly decreased at about
344 26 DAP as the rate of growth slowed (ultimately approaching zero) by the end of the
345 experiment (Fig. 2) while transpiration remained high.

346 We implement two numerical approaches to characterize the genetic
347 architecture of the relationship between these traits. The first method, which is
348 hereafter referred to as the water use efficiency ratio (WUE_{ratio}), calculated the ratio
349 of biomass relative to the volume of water lost from the pot. This calculation was
350 performed on a cumulative or daily rate basis.

351

352 Equation 3:

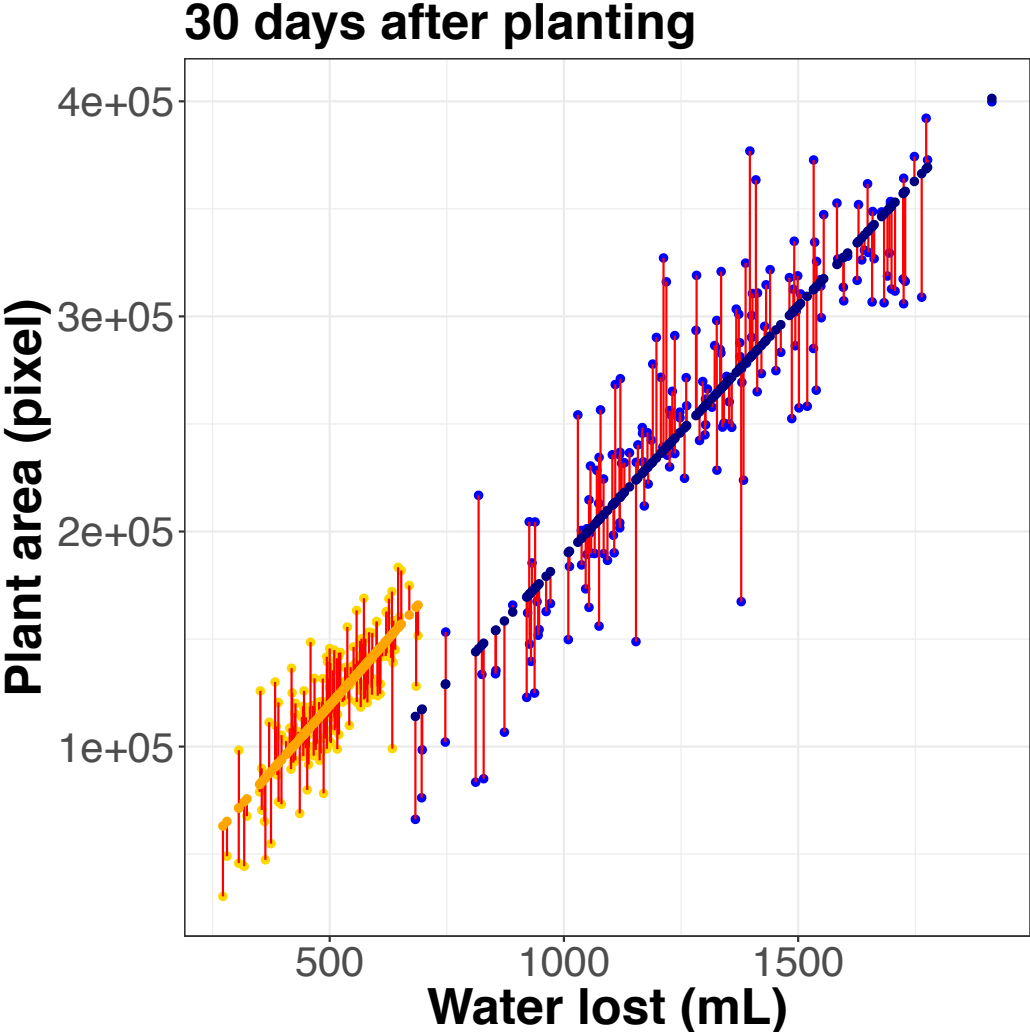
$$353 WUE_{ratio} \text{ (pixel/mL)} = \text{plant size (pixel)} / \text{plant water lost (mL)}$$

354

355 Values of cumulative WUE_{ratio} calculated during this experiment were
356 comparable to other experiments where plant size and water use was measured
357 manually at lower throughput (25-29 grams fresh weight / Liter of water, 7-9 grams
358 dry weight / Liter of water). On average, the cumulative and daily rate WUE_{ratio} was
359 greater in the water-limited treatment block than in well-watered conditions. In
360 principle, the WUE_{ratio} should attenuate the relationship between biomass and water
361 use, but significant correlation was still observed between these two variables,
362 particularly within the rate statistic over the last week of the experiment (Fig. S6,
363 Fig. S7).

364 The high correlation between plant size and water use suggests that they
365 were not independent traits in this experimental setup. Therefore, as a second
366 approach, ordinary least squares linear regression was used to model the
367 relationship between plant biomass and water use. For each day of the experiment,
368 within treatment blocks a WUE_{model} was used to predict plant size
369 (dependent/response variable) based upon water loss (independent/explanatory
370 variable) (Fig. 3). The residual of this model fit was evenly distributed around zero

Figure 3. Modeling the relationship between plant size and water use results in two traits. This approach results in predicted value of water use given size (WUE_{fit}) colored in dark blue and deviations from this relationship ($WUE_{residual}$) plotted in red. Plot illustrates this relationship at 30 days after planting.



371 across the entire distribution of the predicted values suggesting minimal bias of this
372 approach (Fig. S8).

373

374 Equation 4:

375 WUE_{fit} (pixel/mL) = plant size (pixel) \sim water lost (mL) + $WUE_{residual}$ (pixel/mL)

376

377 This approach resulted in two traits: The first was the predicted model fit
378 (WUE_{fit}) that described the sum of squares relationship between biomass and water
379 use. The residual of this model ($WUE_{residual}$) can be thought of as genotype-specific
380 deviation from this relationship combined with measurement error. As expected,
381 the correlation between the fit values derived from the WUE_{model} was highly
382 correlated with plant size (Fig. S9). A slight correlation between cumulative plant
383 biomass and the residual of the WUE_{model} was observed particularly later in the
384 experiment demonstrating that biomass had components that were not accounted
385 for by the linear model fit (Fig. S10). Varying the dependence structure/assignment
386 or fitting of the model using major axis regression framework (Legendre, 2014) had
387 little effect on downstream analysis.

388 Each trait (biomass, water loss, WUE_{ratio} , WUE_{fit} and $WUE_{residual}$) exhibited
389 high average heritability over all experimental time points within and across
390 treatment blocks (0.28 – 0.77) (Fig. S11). Heritability tended to achieve its
391 maximum value in the middle of the experiment with decreased heritability
392 observed at the beginning and the end of the study. Proportionally, the treatment
393 effect of water limitation explained the largest percentage of variance within
394 biomass, water loss and the WUE_{fit} although genotype and genotype x treatment
395 interaction also explain a substantial margin of the variance (Fig. S12). Heritability
396 of the rate traits was generally similar but on average 5% lower than the heritability
397 of the cumulative traits. In all cases, the average heritability of each trait was greater
398 within the well-watered treatment block relative to the value calculated in water-
399 limited treatment block.

400

401 *The genetic architecture of plant size and water use traits*

402 For each day of the experiment, a best fit multiple QTL model was selected
403 for each trait (plant size, water use, WUE_{ratio} , WUE_{fit} and $WUE_{residual}$) and the daily
404 rate of change of the trait within each treatment block based upon penalized LOD
405 score using a standard stepwise forward/backward selection procedure (Broman et
406 al., 2003). This approach identified 86 (cumulative Fig. 4; Table S1) and 106 (rate
407 Fig. S13; Table S1) unique SNPs associated with at least one of the five traits. Many
408 of these uniquely identified SNP positions group into clusters of tightly linked loci
409 that are likely representative of a single QTL location. These local clusters of SNPs
410 (10 cM radius) were then condensed into the most significant marker within each
411 cluster to simplify comparisons of genetic architecture between traits (Fig. S13; Fig.
412 S14). Collapsing these SNP positions yielded 23 unique QTL locations associated
413 with cumulative trait values (Fig. 5) and 27 unique rate QTL locations (Table S2).

414 Of the 23 unique QTL identified, plant biomass contributes the largest
415 proportion of QTL to this set (18) followed by WUE_{ratio} (12), WUE_{fit} (11), $WUE_{residual}$
416 (10) and water lost (8) (Fig. 5, Fig. S16). Despite the fact that only one QTL location
417 (2@96) was common across all traits and environments, the genetic architecture
418 that contributes to each of these characteristics was clearly related. The strong
419 correlation of plant size and water loss with the predicted value of plant size given
420 water loss (WUE_{fit}) are clearly reflected within the genetic architecture associated
421 with these traits. Plant size, water loss and WUE_{fit} all shared 8 QTL (2@96, 3@48,
422 5@109, 6@65, 7@34, 7@51, 7@99 and 9@34) either within the well-watered or
423 water-limited treatment block (Fig. 5, Fig. S16). Plant size, WUE_{ratio} and deviations
424 from the relationship between plant size and water use ($WUE_{residual}$) shared five QTL
425 unique to this subset (2@11, 2@113, 5@79, 5@92, and 9@127) which enable
426 divergence from the fundamental relationship between plant size and water loss
427 (Fig. 5, Fig. S16). Several QTL were identified as being uniquely associated with
428 plant size (3@21, 5@119, 6@80, 9@138), $WUE_{residual}$ (2@82 3@77, 6@47) and
429 WUE_{fit} (5@39) whereas no QTL were identified as being uniquely associated with
430 water loss or WUE_{ratio} (Fig. 5, Fig. S16).

431 The genetic architecture of all five traits appears to be influenced by water
432 availability. All traits other than water loss exhibited QTL unique to each treatment

Figure 4. Eighty-six unique QTL locations were detected across all traits in this experiment.

Each box corresponds to an individual chromosome, where the values along the x-axis are chromosome position and values along the y-axis denote the proportion of genetic variance explained by the QTL. Each triangle represents a single QTL detected, where the color indicates the trait each QTL is associated with (green = plant size, blue = water use, orange = WUE_{ratio} , black = WUE_{fit} , red = $WUE_{residual}$). The darkness of color shading is indicative of treatment block where darker represents well-watered and lighter corresponds to the water-limited block respectively. The direction of the arrow indicates the directional effect of the B100 parental allele.

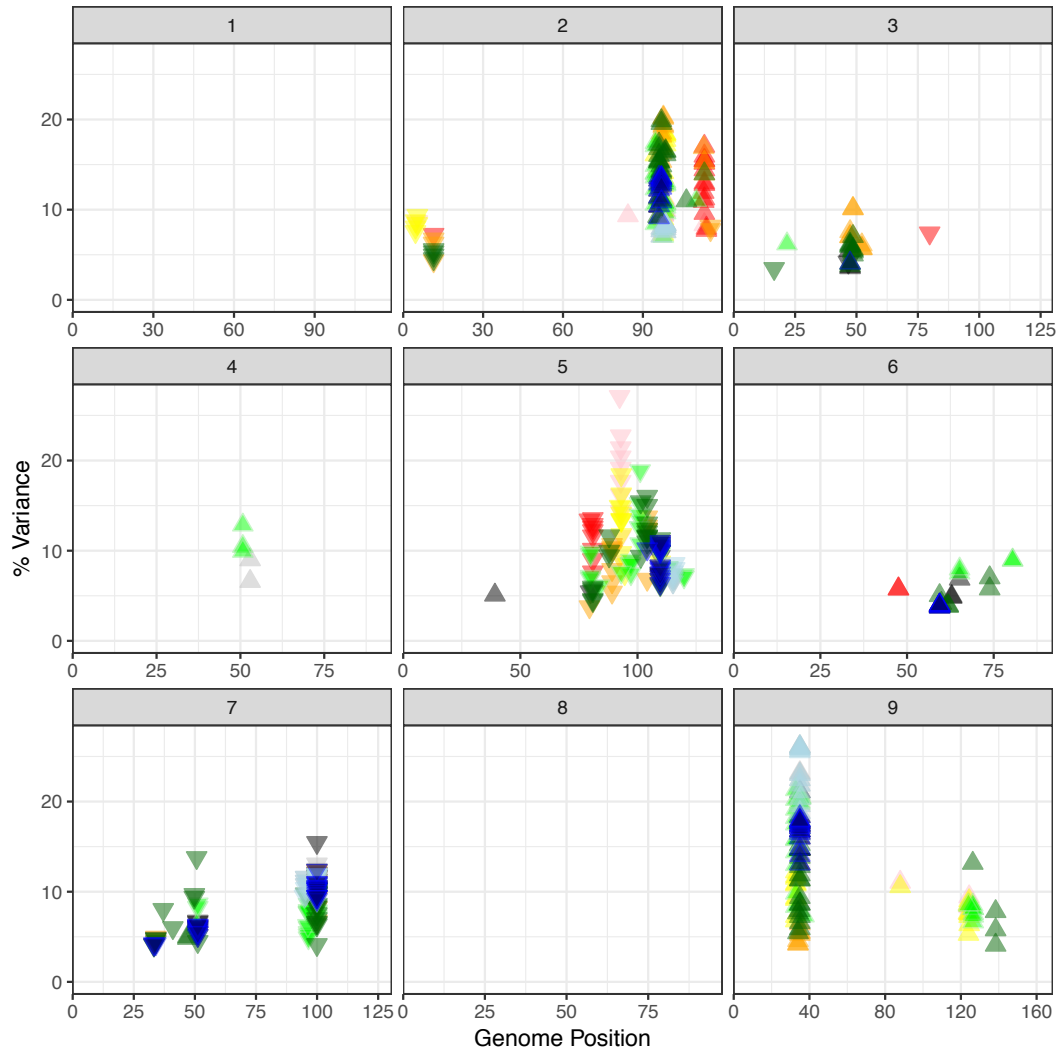
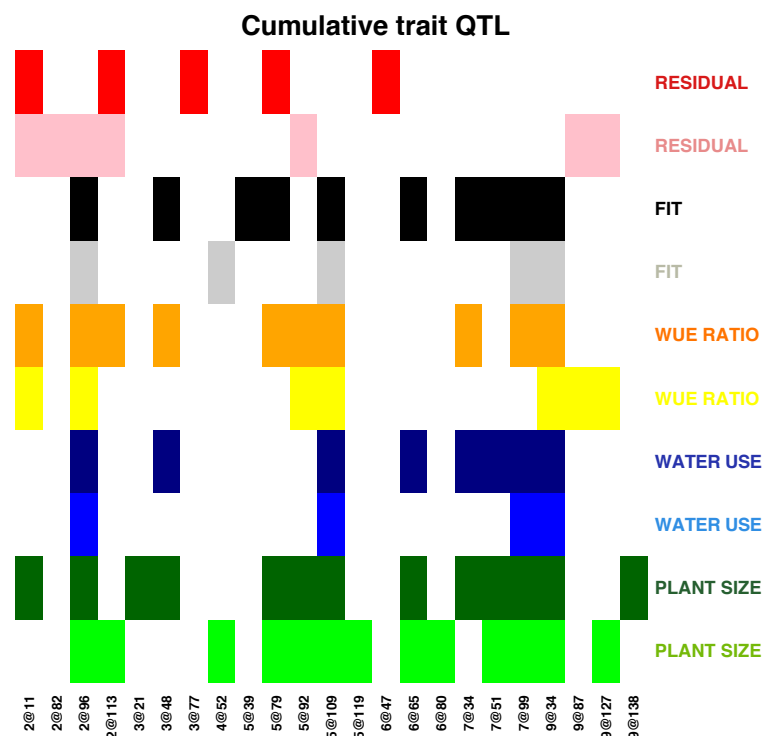


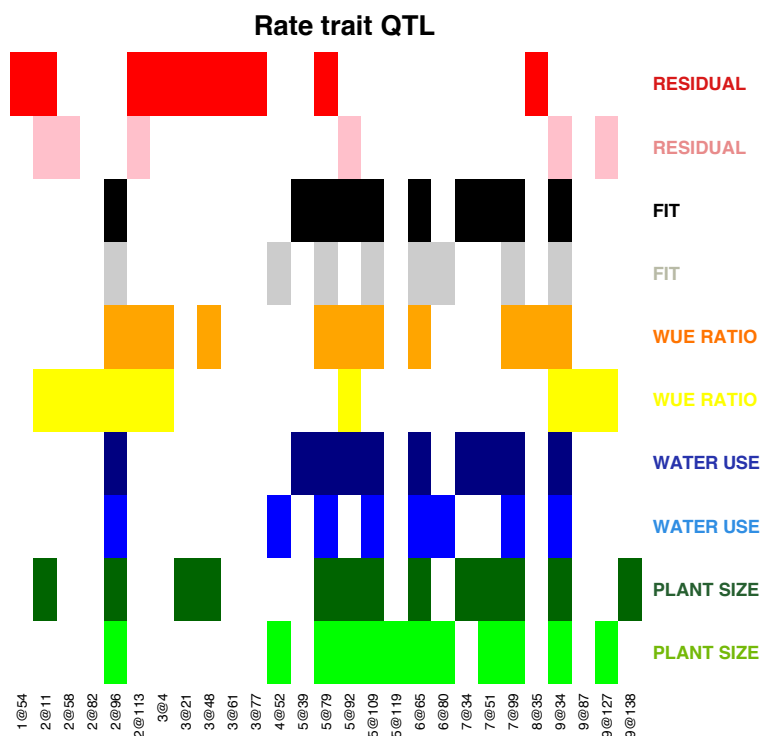
Figure 5. The genetic components that contribute to subsets of traits largely overlap.

The QTL locations identified are plotted on the x-axis and the traits are plotted on the y-axis. Colored matrix entries denote at least one significant association within this experiment. A) The genetic architecture of cumulative traits. B) The genetic loci associated with trait rate of change. C) Genetic components associated with genotype x environment traits.

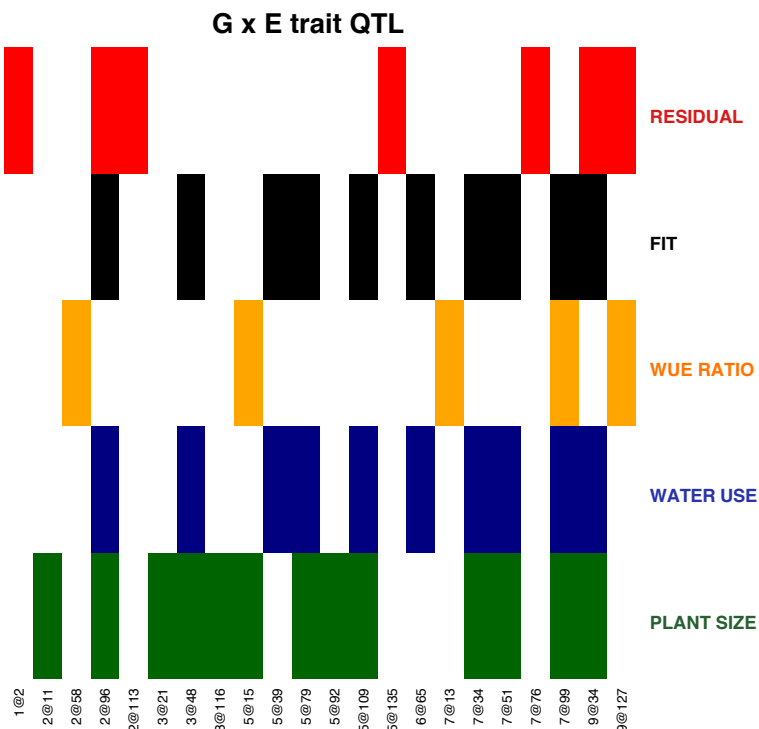
A



B



C



433 block (Fig. 5, Fig. S17). Biomass, water lost, and WUE_{fit} all shared four QTL in
434 common across environments (2@96, 5@109, 7@99 and 9@34) where as WUE_{ratio}
435 and the $WUE_{residual}$ shared a single QTL (2@11) between blocks not found associated
436 with the other traits. Two QTL (3@48, 7@34) were found specifically within the
437 well-watered treatment block for all traits other than $WUE_{residual}$ whereas QTL
438 specific to water-limited environment identified common QTL associated with
439 biomass and WUE_{fit} (4@52) or WUE_{ratio} and $WUE_{residual}$ (9@87, 9@127).

440 The identity of QTL associated with the daily rate values suggest that the
441 genetic architectures were largely cognate with the QTL associated with the traits
442 themselves, both in identity and response to treatment. In total, 28 QTL comprised
443 the union of all unique QTL associated with both the trait value and the daily rate of
444 change calculated from the trait value. Of these QTL, 22 were common between both
445 the trait value and rate statistic associated with the trait, whereas five are only
446 found associated with the rate (1@54, 2@58, 3@4, 3@61, 8@35) and only one QTL
447 was uniquely associated with the cumulative trait values alone (6@47) (Fig. S18).

448

449 *Genotype x environment interactions*

450 To assess the genetic architecture of genotype x environment interactions,
451 mapping was performed on numerical difference, relative difference and trait ratio
452 between the phenotypic values observed within each treatment block. In total, 148
453 unique SNP locations were identified as being significantly associated with at least
454 one of the difference trait formulations across all standard and derived plant size
455 and water use traits (Table S3). Substantial overlap between these categories of
456 genotype x interaction traits indicates that each formulation detects similar genetic
457 signals (Fig. S19) although the large number SNPs found uniquely associated with
458 the trait ratio may indicate that some of these associations may be spurious. As such,
459 these QTL (trait ratio genotype x environment QTL) were removed from further
460 analysis. The numerical difference and relative difference traits exhibited
461 association with 43 and 40 unique SNP positions, which were representative of 20
462 and 18 QTL respectively (Table S4, Fig. S20-22).

463

464 A majority of the QTL (10/15) identified as being associated with the trait
465 difference between treatment blocks were also found associated with the
466 cumulative trait in both treatment blocks (Fig. 5). The exceptions to this were QTL
467 located on 3@21, 3@48, 5@39, 7@34 and 9@127 that were identified as being
468 significantly associated with the difference between treatment blocks but only
469 identified in either well-watered (3@21, 3@48, 5@39, 7@34) or water-limited
470 conditions (9@127). Interestingly, the QTL located on 3@48, 7@34 and 9@127
471 were associated with more than one trait in a single treatment block which may
472 indicate that these QTL impart pleiotropic phenotypic effects that were dependent
473 upon soil water content (Fig. 5).

474

475 *The temporal genetic architecture of plant growth and water usage*

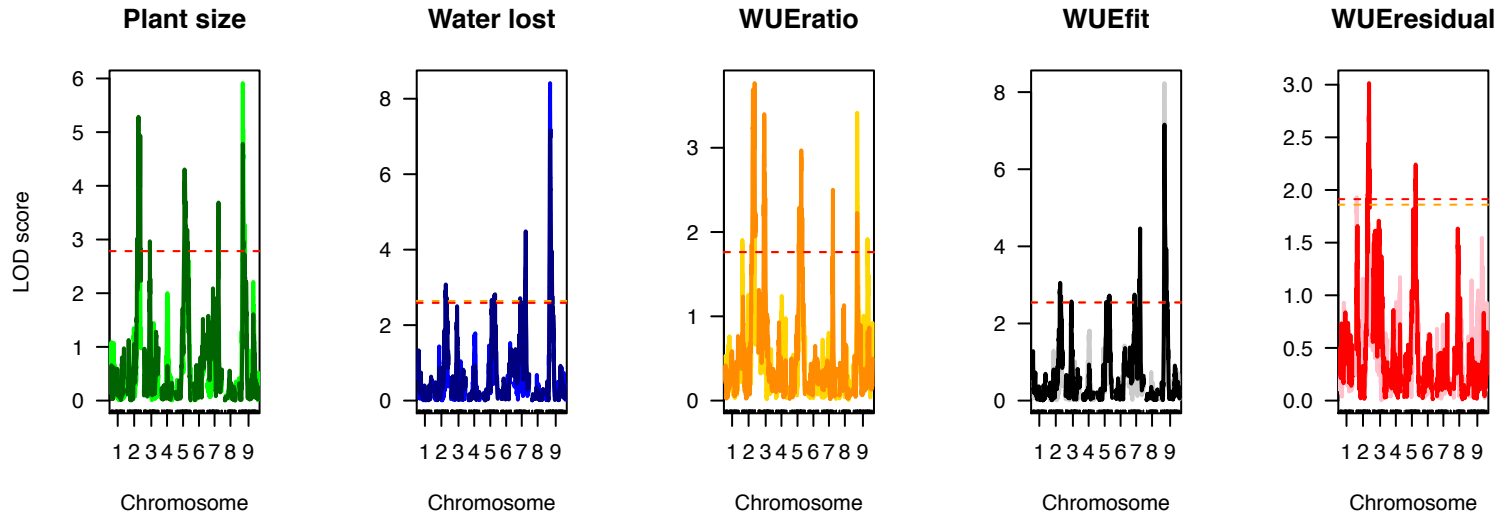
476 In order to account for the time dependence of the traits for the five plant
477 traits, we used a function-valued approach based upon average log-odds score
478 throughout across the experiment (SLOD) for each trait (Kwak et al., 2016). This
479 analysis parallels the individual time point analysis, although the reduction of
480 complexity (fewer, higher confidence QTL) provides an opportunity for
481 simplification and better understanding of the major loci that influence plant WUE.

482 SLOD based function-valued QTL models indicate that several major QTL
483 (2@96, 5@109, 7@99, and 9@36) influenced both plant size and water use related
484 traits, although the magnitude of statistical significance attributed to each loci
485 varied by trait and throughout plant development (Fig. 6, Fig S23). Using the SLOD
486 approach, we were able to partition combinations of QTL unique to related traits
487 (Fig. 6). For several QTL (those around 2@96 and 5@109) the positional location at
488 which maximal LOD score was observed changed noticeably in a trait and
489 environment dependent manner either due to multiple closely linked loci or noise in
490 our measurements. Because the confidence intervals of the QTL generally overlap,
491 our reporting in this section will hereafter refer to these loci by their approximate
492 chromosomal location.

493 Both plant biomass and cumulative water use exhibited almost a complete
494 overlap of QTL within the well-watered treatment block, whereas plant size given

Figure 6. Significant associations identified using single marker scan functional QTL mapping.

Chromosomal position is plotted on the x-axis whereas LOD score of trait association across the genome is plotted on the y-axis. Treatment block is indicated by color intensity (darker is well-watered and lighter is water-limited). Significance thresholds (based on 1000 permutations) are plotted as dashed yellow (water-limited) and red (well-watered) lines respectively.



495 water use (WUE_{fit}) and deviation of plant size from this fundamental relationship
496 ($WUE_{residual}$) each exhibit a unique genetic signature (Fig 6). As observed when trait
497 values at individual time points were treated as independent traits, a single QTL on
498 2@96 is the only genetic component that was shared across all five traits. The linear
499 modeling approach successfully partitions out QTL associated with WUE_{fit} (2@96,
500 7@99, 9@36) from the genetic components that contribute to deviations from the
501 plant size ~ water use relationship ($WUE_{residual}$; 2@96, 5@109). The QTL associated
502 with the WUE_{ratio} (2@96, 3@52, 5@109) also likely reflects deviations from the
503 relationship between biomass given water loss associated with the $WUE_{residual}$.
504 Overall, the identity of QTL associated with each trait was largely identical between
505 the two treatment blocks (Fig. 6, Fig. S23) as were the QTL associated with the
506 values of rate statistics derived from these measurements (Fig. S24, stepwise
507 method; Fig. S25, scanone method).

508

509 *A temporal model of the genetic architecture that influences plant water use efficiency*

510 Our QTL results suggest at least two components of water use efficiency with
511 distinct genetic architectures. In order to compare the genetic architecture across all
512 traits, treatments and time points in a common framework, we analyzed how each
513 trait was influenced by a common set of loci. Fourteen QTL were selected based
514 upon their association with multiple traits, robust linkage with a single trait and/or
515 having differential contribution to traits across treatment blocks (Table S5) and the
516 proportional contribution of each locus to the additive genetic variance was
517 calculated using drop-one-term, type III, ANOVA performed for all experimental
518 traits, time points and treatment. Agglomerative hierarchical clustering of the
519 signed proportion of additive genetic variance explained by each locus was
520 performed to identify modules of traits and loci that define plant phenotypes.
521 Examination of scree plots of the within group sum of squares suggested that the
522 variance within traits could be attributed to approximately six groupings although a
523 majority of this variance could be captured within the largest 2-3 partitions (Fig.
524 S26). These partitions represented the major relationships between trait classes.
525 The WUE_{ratio} and $WUE_{residual}$ were generally grouped separately from a larger cluster

526 of traits that included cumulative plant size, water use and WUE_{fit} (Fig. 7). The
527 genetic architecture of plant water use and WUE_{fit} were more related to each other
528 than they were to plant size, which formed the third group. The influence of water
529 availability on these traits was apparent from the grouping of clusters whereas the
530 effects of time were clear but distributed within the treatment blocks. The genetic
531 architecture of the WUE_{ratio} in the well-watered treatment block at early time points
532 was more similar to the architecture of plant area than itself later in development
533 whereas plant area in the water-limited treatment block exhibited a genetic
534 architecture similar to the WUE_{ratio} late at the end of the experiment.

535 Examination of the signed, proportional allelic effects within the greater fixed
536 QTL model indicated that QTL on 2@96, 5@109, 7@99 and 9@34 contribute
537 medium-to-large effects on a majority of the traits examined in both treatment
538 blocks (Fig. 8). The B100 allele associated with QTL on 2@96 and 9@34 both
539 contributed to increased plant size, water loss, WUE_{fit} and WUE_{ratio} . The QTL on
540 2@96 exhibited its greatest influence in the well-watered treatment block whereas
541 the contribution of 9@34 was greater on average in the water-limited treatment
542 block. Both QTL exhibited similar temporal patterns, showing an earlier effect on
543 plant size and WUE_{ratio} but a consistent effect across water loss. Contribution of the
544 B100 allele on 7@99 and 5@109 decrease plant size, water use and the WUE_{fit}
545 traits; the effect of which was greater in well-watered conditions. The magnitude of
546 effects contributed by QTL on 7@99 on plant size decreased through time whereas
547 the effects on water loss and WUE_{fit} peaked after 20 days and decreases slightly
548 thereafter. The 5@109 locus behaves similarly with little temporal variation in
549 plant water use and WUE_{fit} . A majority of the other QTL contributed minor effects
550 that became more prominent in one of the two treatment blocks or at a particular
551 developmental time points. Inheriting the B100 allele at QTL on 2@113, 3@48,
552 4@52, 6@65 and 9@127 increased the values while the B100 allele at the remaining
553 loci (2@11, 5@79, 5@95, 7@34 and 7@53) decreased the value of the traits (Fig.
554 S27).

555 A majority of the QTL exhibit unidirectional effects across both the well-
556 watered and water-limited treatment blocks although the direction of the effect was

Figure 7. Agglomerative hierarchical clustering defines the relationship between plant size, water use and derived water use efficiency traits.

The additive effect size of fourteen common QTLs was calculated across all traits, treatments and developmental time points through hierarchical clustering using Ward's method. Color bars on the bottom indicate trait (green = plant size, blue = water use, orange = WUE_{ratio} , black = WUE_{fit} , red = $WUE_{residual}$), treatment block (blue = well-watered, orange = water limited), and days after planting (grey scale values where white represents the trait on day 17 and black indicates the trait on day 33).

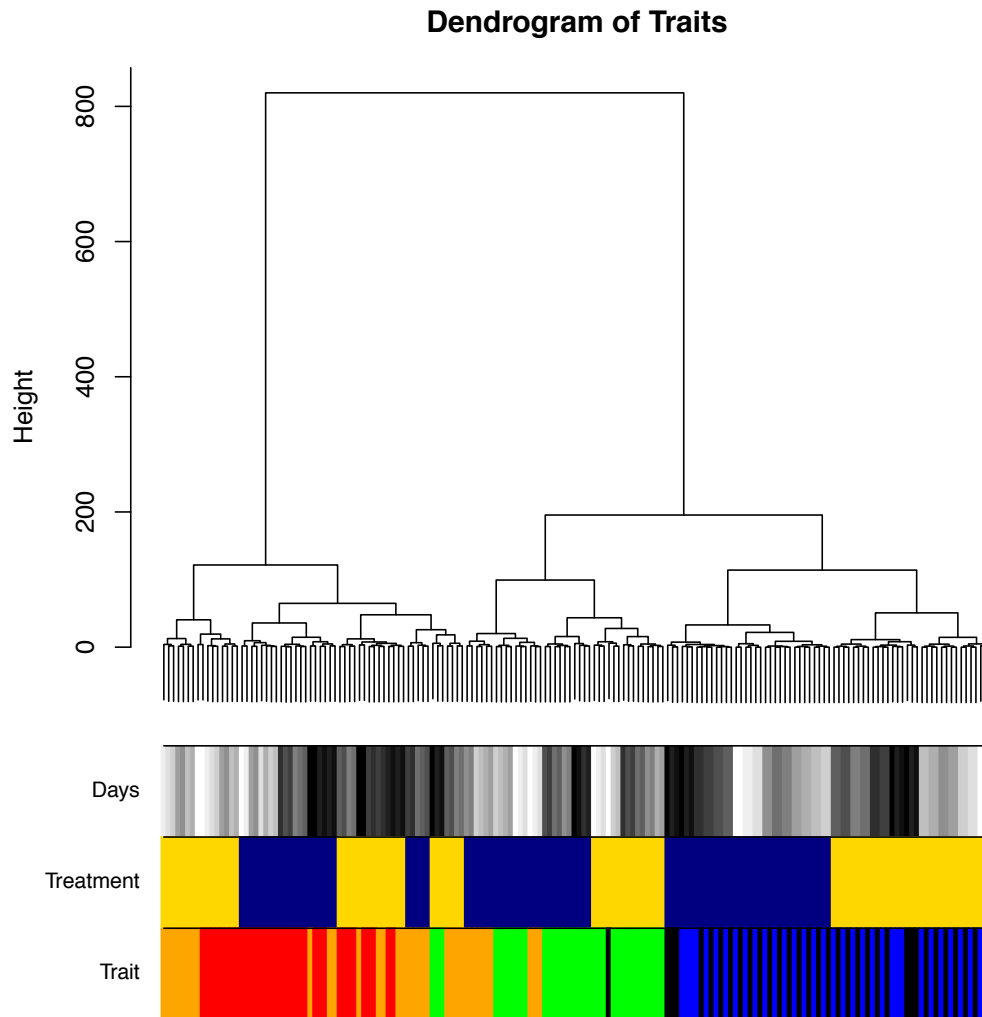
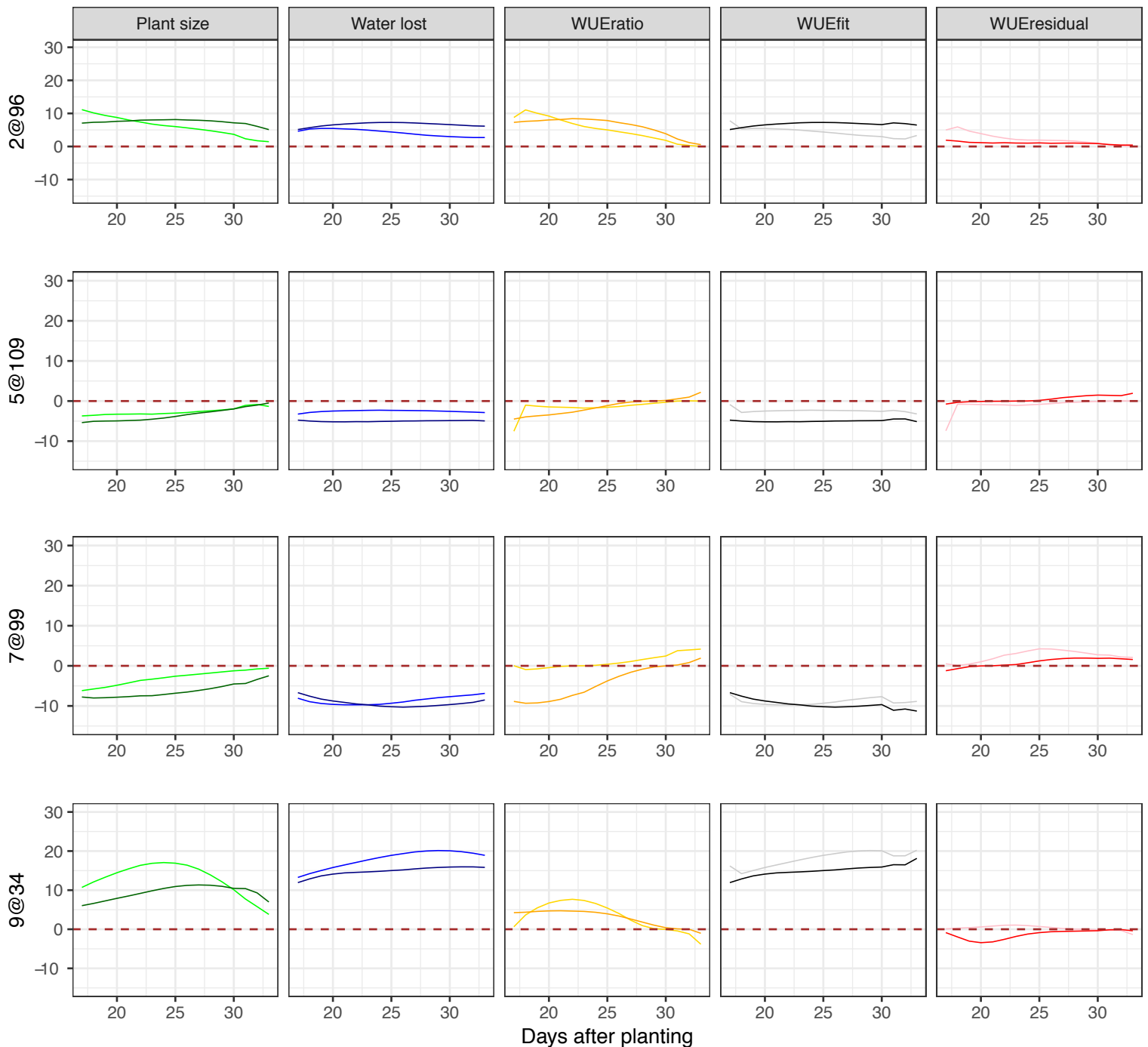


Figure 8. Additive relative effect size of the four major pleiotropic QTL plotted throughout the course of the experiment.

A model containing fourteen QTL was fit across traits, treatment blocks and days. The developmental time point (days after planting) is indicated by the x-axis whereas the proportional additive genetic effect size of the B100 allele is plotted along the y-axis. Columns are representative of traits (green = plant size, blue = water use, orange = WUE_{ratio} , black = WUE_{fit} , red = $WUE_{residual}$) while rows correspond to individual QTL. Shading within the colors denotes treatment block (darker = well-watered, lighter = water-limited).



557 largely dependent on the trait (Fig. S28). The exceptions to this trend represent
558 short periods of experimental time at which the relative effect size is near zero
559 within one or both treatment blocks (Fig. 8, Fig. S27).

560 The proportional contribution of parental alleles towards increased trait
561 values varied between traits, within treatment blocks and throughout plant
562 development. For example, B100 alleles contributed to increased trait values for all
563 traits other than WUE_{ratio} in the water-limited environment and the $WUE_{residual}$
564 across both treatment blocks (Fig. 9). Alternatively, the contributions of the A10
565 alleles proportionally increased the $WUE_{residual}$ value early and then again late in
566 plant development relative to those inherited from the B100 parent. The influence
567 of A10 alleles on the WUE_{ratio} was also greater than their B100 counterpart under water-
568 limited conditions early in plant development.

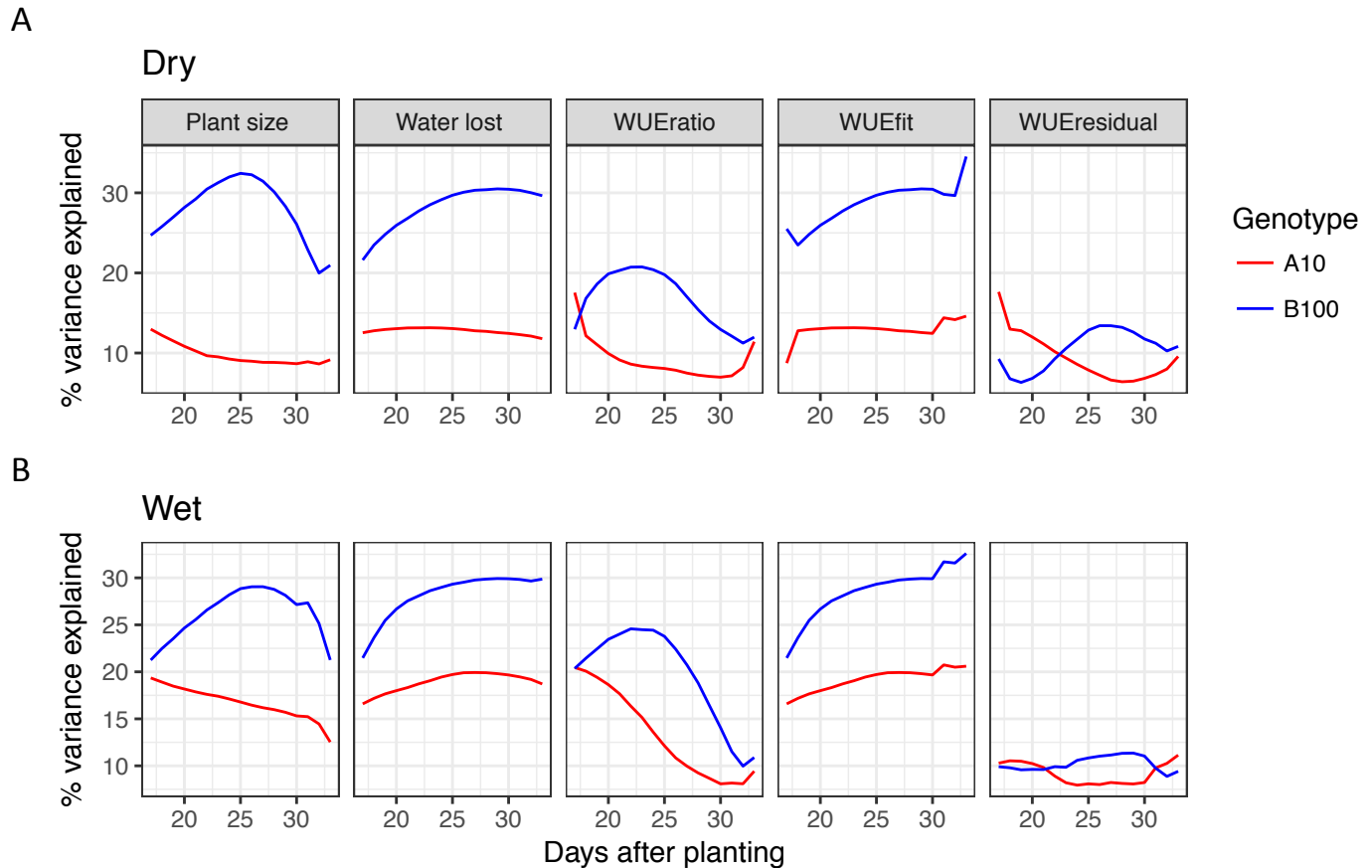
569

570 **DISCUSSION**

571 The objectives of this study were to utilize technological advances in high-
572 throughput phenotyping (Chen et al., 2014; Fahlgren et al., 2015; Granier et al.,
573 2006; Pereyra-Irujo et al., 2012; Reuzeau et al., 2006; Sadok et al., 2007; Tisné et al.,
574 2013; Walter et al., 2007) to characterize the genetic architecture of water use
575 efficiency and how this architecture responds to water-limitation in an experimental
576 C_4 grass model system. Although considerable efforts have been made to
577 characterize these processes in *Arabidopsis thaliana*, C_3 grass crops and other
578 species (Ruggiero et al., 2017) this represents the first study performed on an
579 annual C_4 grass RIL population. These efforts enabled us to identify genetic loci that
580 contribute to differential biomass accumulation given water use in a well-watered
581 and water-limited environment. Our findings suggest that the major genetic
582 components associated with plant size, water use and water use efficiency exhibit
583 pleiotropic behavior and that the magnitude of their allelic effects is dependent
584 upon environment and developmental stage. We used two complementary
585 approaches to define traits, and our analysis confirmed that the genetic architecture
586 was similar with both approaches. We show that the loci controlling biomass
587 accumulation can be roughly divided into two groups: those that control the amount

Figure 9. The proportional contribution of parental alleles to increased trait values depend upon trait, environmental water content and plant developmental stage.

Alleles derived from the B100 parent contribute a greater proportional of additive genetic variance to plant size, water use and TE model fit in both well-watered and water-limited conditions than their A10 allelic counterparts. Both the WUE ratio and TE model residual traits exhibit dynamic behavior where A10 alleles contribute either greater or close to equal proportions of additive genetic variance early and late in plant development. A) The contribution of parental alleles in the water-limited treatment block. B) The contribution of parental alleles in the water-limited treatment block.



588 of water used to create biomass (WUE_{fit}) and those that control how efficiently that
589 water is used ($WUE_{residual}$). The results from this study indicate that alleles from
590 both domesticated foxtail millet and a species representative of its wild progenitor
591 contribute to maximal vegetative biomass yield or water use efficiency grown in
592 environments with different watering regimes. In addition, we highlight aspects of
593 our experimental design and analysis that could be improved in future studies.

594

595 *The genetic architecture of plant size, water use, water use efficiency and the*
596 *relationship between these traits*

597 Within the A10 x B100 *Setaria* RIL population, plant size, water use and the
598 relationship between these two variables are unique polygenic traits whose values
599 are all likely influenced by greater than 10 loci. Four QTL located on 2@96, 5@106,
600 7@99 and 9@36 exhibit strong pleiotropic influence across this suite of traits, the
601 relative magnitude of each is dependent upon growth environment and
602 developmental time point. Despite strong correlation between plant size and water
603 use we successfully identified genetic architectures distinct to each trait. This was
604 achieved by modeling plant size as a function of water use and examining the
605 resulting values of the model fit (plant size given water use) and deviations from
606 this relationship (residual of plant size given water use). This linear modeling
607 approach has been used much less frequently in the literature (Lopez et al., 2015;
608 Nakhforoosh et al., 2016) than the more commonly used WUE_{ratio} (Adiredjo et al.,
609 2014; Honsdorf et al., 2014; Aparna et al., 2015; Fahlgren et al., 2015; Lopez et al.,
610 2015). While the genetic architectures associated with the WUE_{ratio} and $WUE_{residual}$
611 in this population are closely related (Fig. 7), $WUE_{residual}$ exhibits substantial
612 heritability and is less correlated with plant size than the WUE_{ratio} (Fig. S6 Fig. S10),
613 making it a more desirable metric.

614 By examining the model based components of WUE with function valued
615 single marker scan QTL analysis that accounts for multiple hypothesis testing across
616 time points (Kwak et al., 2016), we were able to partition the four major pleiotropic
617 QTL into the genetic components on 2@96, 7@99 and 9@36, which control plant
618 size given water use (WUE_{fit}) and those on 2@96 and 5@109 that contribute to

619 deviations from this relationship ($WUE_{residual}$). This result suggests that QTL
620 associated with WUE_{fit} (7@99 and 9@36) potentially control the development of
621 transpiring plant biomass whereas the QTL associated with the $WUE_{residual}$ and
622 WUE_{ratio} (2@96 and 5@109) influence production of non-transpiring tissues or
623 biological processes not directly related to transpiration. This conclusion is in
624 accordance with the results of other studies performed on this population which
625 demonstrate that these loci are largely pleiotropic (Mauro-Herrera and Doust,
626 2016), although the loci on 2@96 and 5@100 substantially influence plant height
627 (Feldman et al., 2017) and stem biomass, whereas those on 7 and 9 are not
628 associated with the accumulation of stem material (Banan et al., 2017).

629 Our study also identified many smaller effect QTL which influence biomass,
630 water use and WUE traits. The B100 parental allele contributes substantial positive
631 (3@48, 4@52, 6@65, 9@127) and negative (7@34, 7@53) effects on all traits,
632 whereas QTL on 2@11, 2@113, 5@79 and 5@95 contribute either to plant
633 size/ WUE_{ratio} / $WUE_{residual}$ ratio to a greater degree than on plant size/water
634 loss/ WUE_{fit} .

635 Roughly two thirds of the QTL associated with trait plasticity as a response to
636 water availability (difference or relative difference between treatment blocks) were
637 also identified as being associated with the cumulative traits within both treatment
638 blocks. This observation indicates that in many cases, soil water content influences
639 the temporal dynamics of the allelic effects by differential progression through
640 developmental processes that share similar genetic components (Feldman et al.,
641 2017). This study identifies several QTL (3@48, 7@34 and 9@127) associated with
642 genotype by environment traits which also exhibit significant influence on multiple
643 plant traits within a single treatment block. This provides relatively strong evidence
644 that these QTL have pleiotropic influence on size and water use related traits in an
645 environment specific manner. In contrast, QTL identified only by mapping on the
646 difference or relative difference of the traits between each environment are largely
647 specific to individual traits.

648 Evidence from this study supports an evolutionary genetic model where the
649 majority of QTL associated with the measured traits exhibit conditional neutrality

650 across both soil water potentials examined. Although all traits other than plant size
651 sometimes exhibit opposite directional effects across treatment blocks, the evidence
652 supporting a model of antagonistic pleiotropy is weak. When identified, QTL
653 exhibiting opposite directional effects within individual treatment blocks were
654 limited to short periods of experimental time and are characterized by negligible
655 relative effects during these time points. The contributions of alleles from both
656 parental lines contribute to increased WUE irrespective of soil water potential,
657 suggesting that neither parent was optimized for WUE. For example, alleles from the
658 A10 parent contribute a greater proportion of additive genetic variance to increased
659 WUE during early development in both well-watered and water-limited
660 environments, (particularly given the WUE_{residual} derivation of WUE) whereas the
661 alleles derived from the B100 parent have greater affect on a majority of the
662 measured traits throughout the time course. The contribution of alleles of both
663 parents to water use efficiency is expected given earlier study performed on the
664 same platform where parental lines showed similar WUE under water-limited
665 conditions (Fahlgren et al., 2015).

666

667 *Considerations when measuring plant size, water use and WUE*

668 As observed in many other studies (Chen et al., 2012; Fahlgren et al., 2015;
669 Ge et al., 2016; Golzarian et al., 2011; Honsdorf et al., 2014; Lopez et al., 2015;
670 Parent et al., 2015), relative plant side-view pixel area provided a robust and
671 accurate proximity measurement of plant biomass. Although incorporation of
672 additional plant architectural features can improve estimates of this relationship
673 (Parent et al., 2015), our results indicate that caution should be taken as to not over
674 fit models on ground truth data collected exclusively at the end of the experiment as
675 was performed in this study (Fig. S1).

676 Automated or manual gravimetric measurement of pot weight has proven to
677 be a reliable estimator of plant transpiration but only if the evaporative loss of
678 moisture from soil can be accounted for. Results presented in this study indicate
679 that inclusion of empty pots (or pots that contain plastic plants (Parent et al., 2015)
680 or fabric wicks (Halperin et al., 2017)) is an appropriate empirical method to

681 estimate the experimental time point at which transpiration contributes
682 meaningfully to total pot evapotranspiration (Coupel-Ledru et al., 2016; Lopez et al.,
683 2015; Pereyra-Irujo et al., 2012). Estimation of evapotranspiration after this critical
684 time point has been effectively used by several other groups to identify and
685 eliminate confounding data points collected early during similar experiments
686 (Vasseur et al., 2014; Coupel-Ledru et al., 2016; Ge et al., 2016). Our findings
687 indicate that subtraction of empty pot weight (as performed by (Pereyra-Irujo et al.,
688 2012; Parent et al., 2015; Coupel-Ledru et al., 2016)) may overcorrect for
689 evaporation at early experimental time points even after the point at which plant
690 transpiration contributes substantially to total pot water loss. Although not applied
691 during this experiment, utilization of plastic covering to shield pots from
692 evaporative moisture loss in combination with the approaches discussed above may
693 improve the ability to unambiguously quantify plant transpiration (Aparna et al.,
694 2015; Coupel-Ledru et al., 2016; Ellsworth et al., 2017; Granier et al., 2006; Halperin
695 et al., 2017; Vasseur et al., 2014). In this study, the contribution of plant biomass to
696 overall pot weight was not accounted for during the estimation of plant water use.
697 Although the contribution of plant biomass to pot weight in most experiments
698 performed using *Arabidopsis thaliana* is negligible (Tisné et al., 2010), plant biomass
699 within this *Setaria* RIL population accounted for 12-18% of total average pot water
700 content by the end of the experiment (Fig. S4). Our inability to account for this
701 growth has the undesirable effect of systematically decreasing the soil water
702 content of larger genotypes, although in practice this small change in soil water
703 potential likely has minimal impact on transpiration dynamics of the plants.

704 Strong correlation between plant size and water use was observed in spite of
705 the fact that these traits can potentially be controlled by different physiological
706 mechanisms. A similar trend has also been described in experiments designed to
707 study water use efficiency in *Arabidopsis thaliana*, apple and wheat (Lopez et al.,
708 2015; Nakhforoosh et al., 2016; Schoppach et al., 2016; Parent et al., 2015; Vasseur
709 et al., 2014). The magnitude of this correlation is likely inflated in this study due to
710 the large differences in size between parental lines and segregants within the A10 x
711 B100 RIL population. Future studies aimed at investigating the genetic basis of

712 water use efficiency can attenuate this correlation by selecting parental lines of
713 similar size and flowering times that differ in their rates of transpiration within
714 environments of interest.

715

716 CONCLUSIONS

717 This study leverages recent advances in high-throughput phenotyping and
718 quantitative genetics to identify the genetic loci associated with plant size, water use
719 and water use efficiency in an interspecific RIL population of the model C₄ grass
720 *Setaria*. Our findings indicate that these traits are highly heritable and largely
721 polygenic, although the effects of four major pleiotropic QTL account for a
722 substantial proportion of the variance observed within each trait. Contribution of
723 parental alleles from both the domesticated and wild progenitor lines contribute to
724 maximization of these characteristics. Overall, the underlying genetic architecture of
725 each of these processes is distinct and substantially influenced by soil water content
726 as well as plant developmental stage. In addition, several aspects of our
727 experimental design which could be improved to obtain a better understanding of
728 the genetic components that underlie plant size, water use and water use efficiency
729 in future high-throughput phenotyping studies.

730

731 REFERENCE

- 732 **Adiredjo AL, Navaud O, Muños S, Langlade NB, Lamaze T, Grieu P** (2014)
733 Genetic Control of Water Use Efficiency and Leaf Carbon Isotope
734 Discrimination in Sunflower (*Helianthus annuus* L.) Subjected to Two
735 Drought Scenarios. PLoS ONE **9**: e101218
- 736 **Aparna K, Nepolean T, Srivastava RK, Kholová J, Rajaram V, Kumar S, Rekha**
737 **B, Senthilvel S, Hash CT, Vadez V** (2015) Quantitative trait loci associated
738 with constitutive traits control water use in pearl millet [*Pennisetum*
739 *glaucum* (L.) R. Br.]. Plant Biol **17**: 1073–1084
- 740 **Assouline S, Or D** (2013) Plant Water Use Efficiency over Geological Time –
741 Evolution of Leaf Stomata Configurations Affecting Plant Gas Exchange. PLoS
742 ONE **8**: e67757
- 743 **Bacon M** (2009) Water Use Efficiency in Plant Biology. John Wiley & Sons, New
744 York, NY

- 745 **Banan D, Paul R, Feldman MJ, Holmes M, Schlake H, Baxter I, Leakey ADB**
746 (2017) High fidelity detection of crop biomass QTL from low-cost imaging in
747 the field. doi: 10.1101/150144
- 748 **Bates D, Mächler M, Bolker B, Walker S** (2015) Fitting Linear Mixed-Effects
749 Models Using lme4. J Stat Softw. doi: 10.18637/jss.v067.i01
- 750 **Bennetzen JL, Schmutz J, Wang H, Percifield R, Hawkins J, Pontaroli AC, Estep**
751 **M, Feng L, Vaughn JN, Grimwood J, et al** (2012) Reference genome
752 sequence of the model plant *Setaria*. Nat Biotechnol **30**: 555–561
- 753 **Blatt MR** (2000) Cellular Signaling and Volume Control in Stomatal Movements in
754 Plants. Annu Rev Cell Dev Biol **16**: 221–241
- 755 **Blum A** (2009) Effective use of water (EUW) and not water-use efficiency (WUE) is
756 the target of crop yield improvement under drought stress. Field Crops Res
757 **112**: 119–123
- 758 **Boutraa T** (2010) Improvement of Water Use Efficiency in Irrigated Agriculture: A
759 Review. J Agron **9**: 1–8
- 760 **Boyer JS** (1982) Plant Productivity and Environment. Science **218**: 443–448
- 761 **Bozdogan H** (1987) Model selection and Akaike's Information Criterion (AIC): The
762 general theory and its analytical extensions. Psychometrika **52**: 345–370
- 763 **Brodribb TJ, Feild TS, Jordan GJ** (2007) Leaf Maximum Photosynthetic Rate and
764 Venation Are Linked by Hydraulics. PLANT Physiol **144**: 1890–1898
- 765 **Brodribb TJ, McAdam SAM, Jordan GJ, Feild TS** (2009) Evolution of stomatal
766 responsiveness to CO₂ and optimization of water-use efficiency among land
767 plants. New Phytol **183**: 839–847
- 768 **Broman KW, Wu H, Sen S, Churchill GA** (2003) R/qtl: QTL mapping in
769 experimental crosses. Bioinformatics **19**: 889–890
- 770 **Brutnell TP, Wang L, Swartwood K, Goldschmidt A, Jackson D, Zhu X-G, Kellogg**
771 **E, Van Eck J** (2010) *Setaria viridis*: A Model for C₄ Photosynthesis. Plant Cell
772 **22**: 2537–2544
- 773 **Carmo-Silva AE, Francisco A, Powers SJ, Keys AJ, Ascensao L, Parry MAJ,**
774 **Arrabaca MC** (2009) Grasses of different C₄ subtypes reveal leaf traits
775 related to drought tolerance in their natural habitats: Changes in structure,
776 water potential, and amino acid content. Am J Bot **96**: 1222–1235
- 777 **Chambers JM, Hastie T, eds** (1992) Statistical models in S. Wadsworth &
778 Brooks/Cole Advanced Books & Software, Pacific Grove, Calif

- 779 **Chaves MM** (1991) Effects of Water Deficits on Carbon Assimilation. *J Exp Bot* **42**:
780 1–16
- 781 **Chen D, Neumann K, Friedel S, Kilian B, Chen M, Altmann T, Klukas C** (2014)
782 Dissecting the Phenotypic Components of Crop Plant Growth and Drought
783 Responses Based on High-Throughput Image Analysis. *Plant Cell Online* **26**:
784 4636–4655
- 785 **Chen J, Chang SX, Anyia AO** (2012) Quantitative trait loci for water-use efficiency
786 in barley (*Hordeum vulgare* L.) measured by carbon isotope discrimination
787 under rain-fed conditions on the Canadian Prairies. *Theor Appl Genet* **125**:
788 71–90
- 789 **Condon AG** (2004) Breeding for high water-use efficiency. *J Exp Bot* **55**: 2447–2460
- 790 **Condon AG, Richards RA, Rebetzke GJ, Farquhar GD** (2002) Improving Intrinsic
791 Water-Use Efficiency and Crop Yield. *Crop Sci* **42**: 122–131
- 792 **Coupel-Ledru A, Lebon E, Christophe A, Gallo A, Gago P, Pantin F, Doligez A,**
793 **Simonneau T** (2016) Reduced nighttime transpiration is a relevant breeding
794 target for high water-use efficiency in grapevine. *Proc Natl Acad Sci* **113**:
795 8963–8968
- 796 **Davies WJ, Bennett MJ** (2015) Achieving more crop per drop. *Nat Plants* **1**: 15118
- 797 **Des Marais DL, Hernandez KM, Juenger TE** (2013) Genotype-by-Environment
798 Interaction and Plasticity: Exploring Genomic Responses of Plants to the
799 Abiotic Environment. *Annu Rev Ecol Evol Syst* **44**: 5–29
- 800 **Des Marais DL, Razzaque S, Hernandez KM, Garvin DF, Juenger TE** (2016)
801 Quantitative trait loci associated with natural diversity in water-use
802 efficiency and response to soil drying in *Brachypodium distachyon*. *Plant Sci*
803 **251**: 2–11
- 804 **Devos KM, Wang ZM, Beales J, Sasaki T, Gale MD** (1998) Comparative genetic
805 maps of foxtail millet (*Setaria italica*) and rice (*Oryza sativa*). *Theor Appl*
806 *Genet* **96**: 63–68
- 807 **Easlon HM, Nemali KS, Richards JH, Hanson DT, Juenger TE, McKay JK** (2014)
808 The physiological basis for genetic variation in water use efficiency and
809 carbon isotope composition in *Arabidopsis thaliana*. *Photosynth Res* **119**:
810 119–129
- 811 **Edwards CE, Ewers BE, McClung CR, Lou P, Weinig C** (2012) Quantitative
812 Variation in Water-Use Efficiency across Water Regimes and Its Relationship
813 with Circadian, Vegetative, Reproductive, and Leaf Gas-Exchange Traits. *Mol*
814 *Plant* **5**: 653–668

- 815 **Ellsworth PZ, Ellsworth PV, Cousins AB** (2017) Relationship of leaf oxygen and
816 carbon isotopic composition with transpiration efficiency in the C4 grasses
817 *Setaria viridis* and *Setaria italica*. *J Exp Bot* **68**: 3513–3528
- 818 **Escalona JM, Tomàs M, Martorell S, Medrano H, Ribas-Carbo M, Flexas J** (2012)
819 Carbon balance in grapevines under different soil water supply: importance
820 of whole plant respiration: Carbon balance in grapevine. *Aust J Grape Wine*
821 *Res* **18**: 308–318
- 822 **Evans RG, Sadler EJ** (2008) Methods and technologies to improve efficiency of
823 water use: INCREASING WATER USE EFFICIENCIES. *Water Resour Res.* doi:
824 10.1029/2007WR006200
- 825 **Fahlgren N, Feldman M, Gehan MA, Wilson MS, Shyu C, Bryant DW, Hill ST,**
826 **McEntee CJ, Warnasooriya SN, Kumar I, et al** (2015) A Versatile
827 Phenotyping System and Analytics Platform Reveals Diverse Temporal
828 Responses to Water Availability in *Setaria*. *Mol Plant* **8**: 1520–1535
- 829 **Farquhar GD, Hubick KT, Condon AG, Richards RA** (1989) Carbon Isotope
830 Fractionation and Plant Water-Use Efficiency. *In* PW Rundel, JR Ehleringer,
831 KA Nagy, eds, *Stable Isot. Ecol. Res.* Springer New York, New York, NY, pp 21–
832 40
- 833 **Feldman MJ, Paul RE, Banan D, Barrett JF, Sebastian J, Yee M-C, Jiang H, Lipka**
834 **AE, Brutnell TP, Dinneny JR, et al** (2017) Time dependent genetic analysis
835 links field and controlled environment phenotypes in the model C4 grass
836 *Setaria*. *PLOS Genet* **13**: e1006841
- 837 **Fleury D, Jefferies S, Kuchel H, Langridge P** (2010) Genetic and genomic tools to
838 improve drought tolerance in wheat. *J Exp Bot* **61**: 3211–3222
- 839 **Flood PJ, Harbinson J, Aarts MGM** (2011) Natural genetic variation in plant
840 photosynthesis. *Trends Plant Sci* **16**: 327–335
- 841 **Franks PJ, Farquhar GD** (2006) The Mechanical Diversity of Stomata and Its
842 Significance in Gas-Exchange Control. *PLANT Physiol* **143**: 78–87
- 843 **Ge Y, Bai G, Stoerger V, Schnable JC** (2016) Temporal dynamics of maize plant
844 growth, water use, and leaf water content using automated high throughput
845 RGB and hyperspectral imaging. *Comput Electron Agric* **127**: 625–632
- 846 **Golzarian MR, Frick RA, Rajendran K, Berger B, Roy S, Tester M, Lun DS** (2011)
847 Accurate inference of shoot biomass from high-throughput images of cereal
848 plants. *Plant Methods* **7**: 2
- 849 **Granier C, Aguirrezabal L, Chenu K, Cookson SJ, Dauzat M, Hamard P, Thioux J-**
850 **J, Rolland G, Bouchier-Combaud S, Lebaudy A, et al** (2006) PHENOPSIS, an

- 851 automated platform for reproducible phenotyping of plant responses to soil
852 water deficit in *Arabidopsis thaliana* permitted the identification of an
853 accession with low sensitivity to soil water deficit. *New Phytol* **169**: 623–635
- 854 **Gregory PJ, George TS** (2011) Feeding nine billion: the challenge to sustainable
855 crop production. *J Exp Bot* **62**: 5233–5239
- 856 **Halperin O, Gebremedhin A, Wallach R, Moshelion M** (2017) High-throughput
857 physiological phenotyping and screening system for the characterization of
858 plant-environment interactions. *Plant J* **89**: 839–850
- 859 **Hamdy A, Ragab R, Scarascia-Mugnozza E** (2003) Coping with water scarcity:
860 water saving and increasing water productivity. *Irrig Drain* **52**: 3–20
- 861 **Hetherington AM, Woodward FI** (2003) The role of stomata in sensing and driving
862 environmental change. *Nature* **424**: 901–908
- 863 **Holloway-Phillips M-M, Brodribb TJ** (2011) Contrasting hydraulic regulation in
864 closely related forage grasses: implications for plant water use. *Funct Plant*
865 *Biol* **38**: 594
- 866 **Honsdorf N, March TJ, Berger B, Tester M, Pillen K** (2014) High-Throughput
867 Phenotyping to Detect Drought Tolerance QTL in Wild Barley Introgression
868 Lines. *PLoS ONE* **9**: e97047
- 869 **Huang P, Shyu C, Coelho CP, Cao Y, Brutnell TP** (2016) *Setaria viridis* as a Model
870 System to Advance Millet Genetics and Genomics. *Front Plant Sci*. doi:
871 10.3389/fpls.2016.01781
- 872 **Huxman TE, Smith MD, Fay PA, Knapp AK, Shaw MR, Loik ME, Smith SD, Tissue**
873 **DT, Zak JC, Weltzin JF, et al** (2004) Convergence across biomes to a
874 common rain-use efficiency. *Nature* **429**: 651–654
- 875 **Kenney AM, McKay JK, Richards JH, Juenger TE** (2014) Direct and indirect
876 selection on flowering time, water-use efficiency (WUE, $\delta^{13}C$), and WUE
877 plasticity to drought in *Arabidopsis thaliana*. *Ecol Evol* **4**: 4505–4521
- 878 **Kwak I-Y, Moore CR, Spalding EP, Broman KW** (2016) Mapping Quantitative Trait
879 Loci Underlying Function-Valued Traits Using Functional Principal
880 Component Analysis and Multi-Trait Mapping. *G3* **6**: 58
881 *GenesGenomesGenetics* **6**: 79–86
- 882 **Lawson T, Blatt MR** (2014) Stomatal Size, Speed, and Responsiveness Impact on
883 Photosynthesis and Water Use Efficiency. *PLANT Physiol* **164**: 1556–1570

- 884 **Lawson T, von Caemmerer S, Baroli I** (2010) Photosynthesis and Stomatal
885 Behaviour. *In* UE Lüttge, W Beyschlag, B Büdel, D Francis, eds, Prog. Bot. 72.
886 Springer Berlin Heidelberg, Berlin, Heidelberg, pp 265–304
- 887 **Lawson T, Kramer DM, Raines CA** (2012) Improving yield by exploiting
888 mechanisms underlying natural variation of photosynthesis. *Curr Opin*
889 *Biotechnol* **23**: 215–220
- 890 **Legendre P** (2014) lmodel2: Model II Regression. R package version 1.7-2.
- 891 **Li P, Brutnell TP** (2011) *Setaria viridis* and *Setaria italica*, model genetic systems
892 for the Panicoid grasses. *J Exp Bot* **62**: 3031–3037
- 893 **Lopez G, Pallas B, Martinez S, Lauri P-É, Regnard J-L, Durel C-É, Costes E** (2015)
894 Genetic Variation of Morphological Traits and Transpiration in an Apple Core
895 Collection under Well-Watered Conditions: Towards the Identification of
896 Morphotypes with High Water Use Efficiency. *PLOS ONE* **10**: e0145540
- 897 **Lowry DB, Logan TL, Santuari L, Hardtke CS, Richards JH, DeRose-Wilson LJ,**
898 **McKay JK, Sen S, Juenger TE** (2013) Expression Quantitative Trait Locus
899 Mapping across Water Availability Environments Reveals Contrasting
900 Associations with Genomic Features in *Arabidopsis*. *Plant Cell* **25**: 3266–
901 3279
- 902 **Martre P, Cochard H, Durand J-L** (2001) Hydraulic architecture and water flow in
903 growing grass tillers (*Festuca arundinacea* Schreb.). *Plant Cell Environ* **24**:
904 65–76
- 905 **Mauro-Herrera M, Doust AN** (2016) Development and Genetic Control of Plant
906 Architecture and Biomass in the Panicoid Grass, *Setaria*. *PLOS ONE* **11**:
907 e0151346
- 908 **Mojica JP, Mullen J, Lovell JT, Monroe JG, Paul JR, Oakley CG, McKay JK** (2016)
909 Genetics of water use physiology in locally adapted *Arabidopsis thaliana*.
910 *Plant Sci* **251**: 12–22
- 911 **Monteith JL** (1993) The exchange of water and carbon by crops in a mediterranean
912 climate. *Irrig Sci*. doi: 10.1007/BF00208401
- 913 **Morison JI., Baker N., Mullineaux P., Davies W.** (2008) Improving water use in
914 crop production. *Philos Trans R Soc B Biol Sci* **363**: 639–658
- 915 **Nakhforoosh A, Bodewein T, Fiorani F, Bodner G** (2016) Identification of Water
916 Use Strategies at Early Growth Stages in Durum Wheat from Shoot
917 Phenotyping and Physiological Measurements. *Front Plant Sci*. doi:
918 10.3389/fpls.2016.01155

- 919 **Parent B, Shahinnia F, Maphosa L, Berger B, Rabie H, Chalmers K, Kovalchuk A,**
920 **Langridge P, Fleury D** (2015) Combining field performance with controlled
921 environment plant imaging to identify the genetic control of growth and
922 transpiration underlying yield response to water-deficit stress in wheat. *J*
923 *Exp Bot* **66**: 5481–5492
- 924 **Pater D, Mullen JL, McKay JK, Schroeder JI** (2017) Screening for Natural Variation
925 in Water Use Efficiency Traits in a Diversity Set of *Brassica napus* L. Identifies
926 Candidate Variants in Photosynthetic Assimilation. *Plant Cell Physiol* **58**:
927 1700–1709
- 928 **Penman H, Schofield R** (1951) Some physical aspects of assimilation and
929 transpiration. *Carbon Dioxide Fixat. Photosynth.* 5:
- 930 **Pereyra-Irujo GA, Gasco ED, Peirone LS, Aguirrezábal LAN** (2012) GlyPh: a low-
931 cost platform for phenotyping plant growth and water use. *Funct Plant Biol*
932 **39**: 905
- 933 **Premachandra GS, Hahn DT, Axtell JD, Joly RJ** (1994) Epicuticular wax load and
934 water-use efficiency in bloomless and sparse-bloom mutants of *Sorghum*
935 *bicolor* L. *Environ Exp Bot* **34**: 293–301
- 936 **Reuzeau C, Frankard V, Hatzfeld Y, Sanz A, Van Camp W, Lejeune P, De Wilde C,**
937 **Lievens K, de Wolf J, Vranken E, et al** (2006) Traitmill™: a functional
938 genomics platform for the phenotypic analysis of cereals. *Plant Genet Resour*
939 *Charact Util* **4**: 20–24
- 940 **Ruggiero A, Punzo P, Landi S, Costa A, Van Oosten M, Grillo S** (2017) Improving
941 Plant Water Use Efficiency through Molecular Genetics. *Horticulturae* **3**: 31
- 942 **Ryan AC, Dodd IC, Rothwell SA, Jones R, Tardieu F, Draye X, Davies WJ** (2016)
943 Gravimetric phenotyping of whole plant transpiration responses to
944 atmospheric vapour pressure deficit identifies genotypic variation in water
945 use efficiency. *Plant Sci* **251**: 101–109
- 946 **Sack L, Holbrook NM** (2006) LEAF HYDRAULICS. *Annu Rev Plant Biol* **57**: 361–381
- 947 **Sadok W, Naudin P, Boussuge B, Muller B, Welcker C, Tardieu F** (2007) Leaf
948 growth rate per unit thermal time follows QTL-dependent daily patterns in
949 hundreds of maize lines under naturally fluctuating conditions. *Plant Cell*
950 *Environ* **30**: 135–146
- 951 **Saha P, Sade N, Arzani A, Rubio Wilhelmi M del M, Coe KM, Li B, Blumwald E**
952 (2016) Effects of abiotic stress on physiological plasticity and water use of
953 *Setaria viridis* (L.). *Plant Sci* **251**: 128–138

- 954 **Schoppach R, Taylor JD, Majerus E, Claverie E, Baumann U, Suchecki R, Fleury**
955 **D, Sadok W** (2016) High resolution mapping of traits related to whole-plant
956 transpiration under increasing evaporative demand in wheat. *J Exp Bot* **67**:
957 2847–2860
- 958 **Seibt U, Rajabi A, Griffiths H, Berry JA** (2008) Carbon isotopes and water use
959 efficiency: sense and sensitivity. *Oecologia* **155**: 441–454
- 960 **Stanhill G** (1986) Water Use Efficiency. *Adv. Agron.* Elsevier, pp 53–85
- 961 **Stewart G, Turnbull M, Schmidt S, Erskine P** (1995) ¹³C Natural Abundance in
962 Plant Communities Along a Rainfall Gradient: a Biological Integrator of Water
963 Availability. *Aust J Plant Physiol* **22**: 51
- 964 **Tardieu F** (2013) Plant response to environmental conditions: assessing potential
965 production, water demand, and negative effects of water deficit. *Front*
966 *Physiol.* doi: 10.3389/fphys.2013.00017
- 967 **Tisné S, Schmalenbach I, Reymond M, Dauzat M, Pervent M, Vile D, Granier C**
968 (2010) Keep on growing under drought: genetic and developmental bases of
969 the response of rosette area using a recombinant inbred line population: Leaf
970 development and drought stress. *Plant Cell Environ* **33**: 1875–1887
- 971 **Tisné S, Serrand Y, Bach L, Gilbault E, Ben Ameer R, Balasse H, Voisin R,**
972 **Bouchez D, Durand-Tardif M, Guerche P, et al** (2013) Phenoscope: an
973 automated large-scale phenotyping platform offering high spatial
974 homogeneity. *Plant J* **74**: 534–544
- 975 **Tomás M, Medrano H, Escalona JM, Martorell S, Pou A, Ribas-Carbó M, Flexas J**
976 (2014) Variability of water use efficiency in grapevines. *Environ Exp Bot*
977 **103**: 148–157
- 978 **Vasseur F, Bontpart T, Dauzat M, Granier C, Vile D** (2014) Multivariate genetic
979 analysis of plant responses to water deficit and high temperature revealed
980 contrasting adaptive strategies. *J Exp Bot* **65**: 6457–6469
- 981 **Walter A, Scharr H, Gilmer F, Zierer R, Nagel KA, Ernst M, Wiese A, Virnich O,**
982 **Christ MM, Uhlig B, et al** (2007) Dynamics of seedling growth acclimation
983 towards altered light conditions can be quantified via GROWSCREEN: a setup
984 and procedure designed for rapid optical phenotyping of different plant
985 species. *New Phytol* **174**: 447–455
- 986 **Wang ZM, Devos KM, Liu CJ, Wang RQ, Gale MD** (1998) Construction of RFLP-
987 based maps of foxtail millet, *Setaria italica* (L.) P. Beauv. *Theor Appl Genet*
988 **96**: 31–36

- 989 **White TA, Snow VO** (2012) A modelling analysis to identify plant traits for
990 enhanced water-use efficiency of pasture. *Crop Pasture Sci* **63**: 63
- 991 **Winter K, Aranda J, Holtum JAM** (2005) Carbon isotope composition and water-
992 use efficiency in plants with crassulacean acid metabolism. *Funct Plant Biol*
993 **32**: 381
- 994 **Xu Y, This D, Pausch RC, Vonhof WM, Coburn JR, Comstock JP, McCouch SR**
995 (2009) Leaf-level water use efficiency determined by carbon isotope
996 discrimination in rice seedlings: genetic variation associated with population
997 structure and QTL mapping. *Theor Appl Genet* **118**: 1065–1081
- 998 **Zegada-Lizarazu W, Iijima M** (2005) Deep Root Water Uptake Ability and Water
999 Use Efficiency of Pearl Millet in Comparison to Other Millet Species. *Plant*
1000 *Prod Sci* **8**: 454–460
- 1001 **Zhou Y, Lambrides CJ, Kearns R, Ye C, Fukai S** (2012) Water use, water use
1002 efficiency and drought resistance among warm-season turfgrasses in shallow
1003 soil profiles. *Funct Plant Biol* **39**: 116
- 1004 **Zhu C, Yang J, Shyu C** (2017) *Setaria Comes of Age: Meeting Report on the Second*
1005 *International Setaria Genetics Conference*. *Front Plant Sci*. doi:
1006 [10.3389/fpls.2017.01562](https://doi.org/10.3389/fpls.2017.01562)
- 1007